Erciyes Üniversitesi
Fen Bilimleri Enstitüsü Dergisi
Cilt 35, Sayı 1, 2019

Erciyes University
Journal of Institue Of Science and Technology
Volume 35, Issue 1, 2019

MRI Kontrast Maddelerinin Gelişimi için Kuantum Kimyasal ve QSAR Çalışmaları

Murat Saraçoğlu*[1], Sedat Giray Kandemirli[2], Hakan Sezgin Sayiner[3], Murat Alper Başaran[4], Fatma Kandemirli[5]

***[1]Erciyes University, Faculty of Education, 38039, Kayseri, Turkey**
[2]Uludag University, Faculty of Medicine Radiology Department, 16059, Bursa, Turkey
[3]Adıyaman University, Faculty of Medicine, Department of Infectious Diseases, 02040, Adıyaman, Turkey
[4]Alanya Alaaddin Keykubat University, Faculty of Engineering, Department of Management Engineering, 07425, Antalya, Turkey
[5]Kastamonu University, Faculty of Engineering and Architecture, Biomedical Engineering Department, 37150, Kastamonu, Turkey

(Alınış / Received: 29.01.2019, Kabul / Accepted: 17.02.2019, Online Yayınlanma / Published Online: 30.04.2019)

Anahtar Kelimeler
Polyamino-polikarboksilik ligandlar,
MRI Kontrast Ajanlar,
DFT,
B3LYP,
Kuantum kimyasal hesaplamalar,
İstatistiksel analiz.

Öz: Bileşiklerin stabilitesini belirlemek için poliamino-polikarboksilik ligandları çalıştık. Bileşikler, Gaussian Program kullanılarak B3LYP / 6-311G(d,p) ve B3LYP / 6-311 ++ G(d,p) teorisi ile hesaplanmıştır. Tüm istatistiksel analizler sırasıyla; Mat Lab 7.9 ve SPSS 20.0 adı verilen iki farklı yazılım kullanılarak gerçekleştirilmiştir. Gd (III) komplekslerinin kararlılık sabitlerinin tahmini için 37 poliamino-polikarboksilik ligandlarının için E_{HOMO}, E_{LUMO}, E_{HOMO} ve E_{LUMO} arasındaki enerji farkı (ΔE), iyonlaşma enerjisi (IE), mutlak elektronegatiflik (χ), mutlak sertlik (η), yumuşaklık (σ) gibi elektronik ve moleküler özellikler nötr moleküller için gaz fazı için DFT/B3LYP/6-311G(d,p) ve 6-311++ G(2d,2p) yöntemleri ile hesaplanmıştır.

The Quantum Chemical and QSAR Studies for the Development of MRI Contrast

Keywords
Polyamino-polycarboxylic ligands,
MRI Contrast Agents,
DFT,
B3LYP,
Quantum chemical calculations,
Statistical analysis

Abstract: We have studied polyamino-polycarboxylic ligands to determine the stability of the compounds. The compounds were calculated with the theory of B3LYP/6-311G(d,p) and B3LYP/6-311++G(d,p) by using Gaussian Program. All statistical analysis was conducted employing two different soft wares called Mat Lab 7.9 and SPSS 20.0, respectively. The electronic and molecular properties, such as the polarizability, E_{HOMO}, E_{LUMO}, the energy gap between E_{HOMO} and E_{LUMO} (ΔE), İonization energy (IE), absolute electronegativity (χ), absolute hardness (η), softness (σ), of 37 polyamino-polycarboxylic ligands for prediction of stability constants of Gd(III) complexes were calculated with the DFT/B3LYP/6-311G(d,p) and 6-311++G(2d,2p) methods for gas phase for neutral molecules.

1. Introduction

The lanthanide series fall into a category called ‘‘hard’’ acids due to bonding with other elements is considered largely ionic or electrostatic. Gd^{3+} is toxic in biological systems due to having an ionic radius of 0.99 Å and very

nearly equal to that of divalent Ca^{2+}. Gd^{3+} can make 8–9 inner-sphere water molecules each contributing a small amount of electron density to the highly charged Gd^{3+} ion, as a hydrated ''aqua'' ion below pH-6. When Gd ion makes chelation with ligands, ligands are placed instead of some of the water molecules. Ligands have more basic donor atoms such as amines (N) or carboxylates (O). The factors that affect the stability of the complex are temperature, pH, the structure of the ligand, charges on the central metal atom. As a general rule, as a general rule of thumb, Gd^{3+} ion makes the most stable complexes with the most basic donor atoms. Magnetic Resonance Imaging (MRI) contrast agents are used to enhance image contrast and to facilitate the appearance of lesions. Contrast materials used in RG studies are classified into two categories depending on the relaxation process [1-3]. T1 agents shorten the T1 relaxation times, causing the tissues to appear white (bright). T1 agents consist of gadolinium and manganese salts, and T2 agents shorten the T1 relaxation times, causing the tissues to appear white (bright). T2 agents are iron oxide-containing agents. Based on the tissues they act on contrast materials are classified as Nonspecific (extracellular) Agents which are gadolinium contrast agents used in routine MRI applications and tissue specific agents which are produced for targeted organs. These include agents for hepatocytes, agents for early nonspecific-late hepatocytes, agents for the reticuloendothelial system (RES), early-stage blood pools, and late-onset RES agents [4-6].

Gadolinium(III)[4,10-bis-carboxymethyl-7-({3-[3-(4-dimethylaminophenyl)-2-oxo-2*H*-chromen-7-yloxy]-propylcarbamoyl}methyl)-1,4,7,10-tetraazacyclododec-1-yl]-acetate), a myelin-targeting MR agent termed MIC was developed MIC has got coumarin binding moiety. It was demonstrated that MIC binds to myelin sheaths in vitro and in vivo and could be used to characterize myelin distribution based on T1w MR imaging in murine models [6, 7}. Then Gadolinium (E)-2,2′,2″-(10-(2-((3-(4-((4-(4-(methylamino)styryl)phenoxy)methyl)-1*H*-1,2,3-triazol-1-yl)propyl)amino)-2-oxoethyl)-1,4,7,10-tetraazacyclododecane-1,4,7-triyl)triacetic acetate was synthesized a second type of myelin-targeted MR contrast agent bearing an aminostilbene moiety and compound binding to myelin was demonstrated both in vitro and in situ by fluorescent microscopy and in vivo by T1w MR imaging [8]. Porphyrazines (Pz) being a sub-class of tetrapyrrole macrocycles have been investigated for a number of tumor biology applications such as photodynamic therapy and near-infrared optical imaging [9-11]. Second generation Pz-Gd(III) conjugates were synthesized and reported that these compounds were indeed taken up by cells in vitro, warranting extensive in vivo MRI studies in athymic nude mouse tumor models of human breast cancer [12].

The first gadolinium-based contrast agent (GBCA), Gadopentetate dimeglumine (Magnevist) designed for magnetic resonance imaging (MRI) in 1988 and started to be used clinically. The reason for using Gd (III) ion is the appropriate combination of a large magnetic moment (spin-only μeff = ¼ 7.94 BM, from seven half-filled f orbitals) and long electron spin deceleration time (10^{-8} to 10^{-9} s, from symmetric S electronic state) [13]. Gd^{3+} ion, in its free is exceptionally toxic for living systems, is a hard metal ion. It acts as an acceptor and form complexes with ligands.

Kiani-Anbouhi et al performed the quantitative structure-property relationships models for prediction of stability constants of Gd(III) complexes with polyamino-polycarboxylic ligands and they found a good quality of model ($Q2=0.916$ and $R^2=0.935$) enables reliable prediction of stability constants for unmeasured complexes [14].

We have studied polyamino-polycarboxylic ligands to determine the stability of the compounds. The descriptors, such as exact E_{HOMO}, E_{LUMO}, ΔE, chemical hardness, chemical softness, chemical potential, sum of electronic and zero point energies, dipole moment, electronegativity, polarizibility, electrophilicity index of the compounds were calculated with the theory of B3LYP/6-311G(d,p) and B3LYP/6-311++G(d,p) by using Gaussian Program [15]. All statistical analysis was conducted employing two different soft wares called Mat Lab 7.9 and SPSS 20.0, respectively.

2. Material and Method

The molecular sketches of the polyamino-polycarboxylic ligands were drawn using the GaussView 5.0. All the quantum chemical calculations were performed with complete geometry optimizations using the Becke's three-parameter hybrid functional [16-18] combined with the Lee, Yang, and Parr (LYP) correlation functional [19] denoted as B3LYP in the density functional theory with a standard Gaussian-09 software package [15]. 6-311G(d,p) and 6-311++G(2d,2p) basis sets were used for all the quantum chemical calculations. Fukui functions were performed with the AOMix program [20, 21] using single point calculations with the B3LYP/6-311G(d,p) basis sets.

In this study, 37 polyamino-polycarboxylic ligands (see **Table 1**) were chosen to describe the structure of the molecules constituting the series to study/ the highest occupied molecular orbital energy (E_{HOMO}, eV), the lowest unoccupied molecular orbital energy (E_{LUMO}, eV) and other quantum chemical parameters were calculated. Recently, optimization of molecules with different basic sets and discussion of the results are widely used [22-42].

2.1. Computational details

In the section of this study, all calculations were carried out using DFT/B3LYP method. Optimization of synthesized molecules was performed with 6-311G(d,p) and 6-311++G(2d,2p) basis sets of Gaussian program [15]. This basis set is known as one of the basis sets that gives more accurate results in terms of the determination of electronic and geometries properties for a wide range of organic compounds [43]. Quantum chemical parameters for synthesized molecules such as the energy of the highest occupied molecular orbital (E_{HOMO}), the energy of the lowest unoccupied molecular orbital (E_{LUMO}), HOMO-LUMO energy gap (ΔE), ionization energy (IE), chemical hardness (η), softness (σ), electronegativity (χ), chemical potential (μ), dipole moment (DM), global electrophilicity (ω), sum of the total negative charge (TNC) and sum of electronic and zero-point energies (SEZPE) for gas phase of neutral molecules were calculated and discussed.

Molecular properties, related to the reactivity and selectivity of the compounds, were estimated following the Koopmans's theorem relating the energy of the HOMO and the LUMO. According to the DFT-Koopmans' theorem [44], the ionization potential (IE) can be approximated as the negative value of the highest occupied molecular orbital energy (E_{HOMO}), such as shown in equation 1:

$$IE = -E_{HOMO} \quad (1)$$

The negative value of the lowest unoccupied molecular orbital energy (E_{LUMO}) is similarly related to the electron affinity A [45] such as shown in equation 2:

$$A = -E_{LUMO} \quad (2)$$

Electronegativity is estimated using the following the equation from E_{HOMO} and E_{LUMO}:

$$\chi \cong -\frac{1}{2}(E_{HOMO} + E_{LUMO}) \quad (3)$$

Chemical hardness (η) measures the resistance of an atom to a charge transfer [46], it is estimated by using the equation from E_{HOMO} and E_{LUMO}:

$$\eta \cong -\frac{1}{2}(E_{HOMO} - E_{LUMO}) \quad (4)$$

Chemical potential (μ) and electronegativity (χ) can be calculated with the help of the following equations [43] from E_{HOMO} and E_{LUMO}:

$$\mu = -\chi \cong \frac{E_{HOMO}+E_{LUMO}}{2} \quad (5)$$

Electron polarizability, called chemical softness (σ), describes the capacity of an atom or group of atoms to receive electrons [46] and is estimated by using the equation:

$$\sigma = \frac{1}{\eta} \cong -\frac{2}{(E_{HOMO}-E_{LUMO})} \quad (6)$$

The global electrophilicity (ω) is a useful reactivity descriptor that can be used to compare the electron-donating abilities of molecules [47]. Global electrophilicity index is estimated by using the electronegativity and chemical hardness parameters through the equation:

$$\omega = \frac{\chi^2}{2\eta} \quad (7)$$

A high value of electrophilicity describes a good electrophile while a small value of electrophilicity describes a good nucleophile [48].

Table 1. The structure of investigated compounds.

No	Compounds	No	Compounds
1	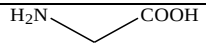	**24**	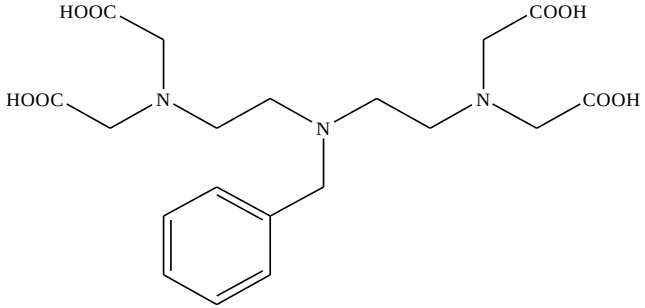
2	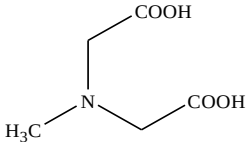		
3	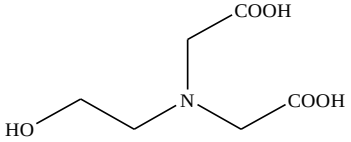		
4	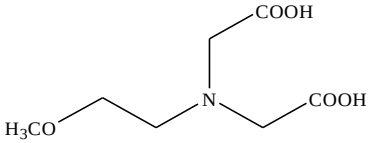	**25**	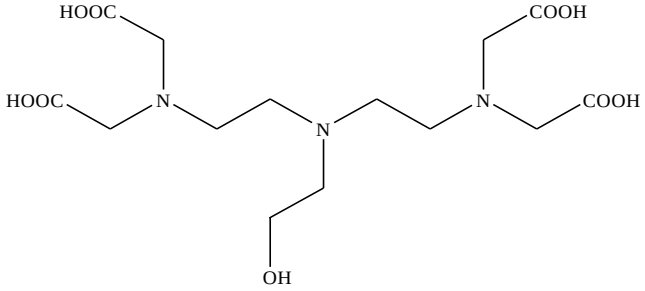
5	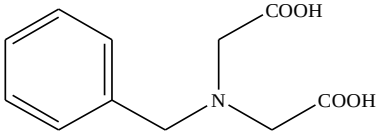		
6	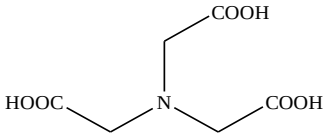	**26**	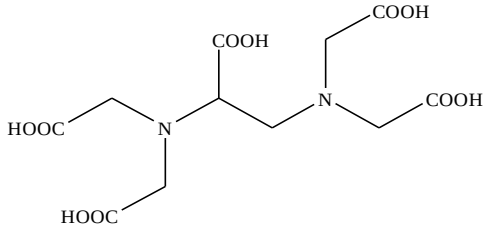
7	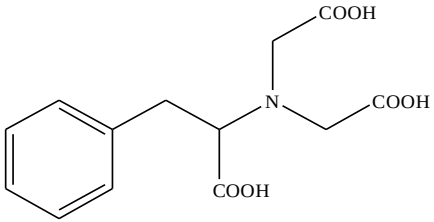	**27**	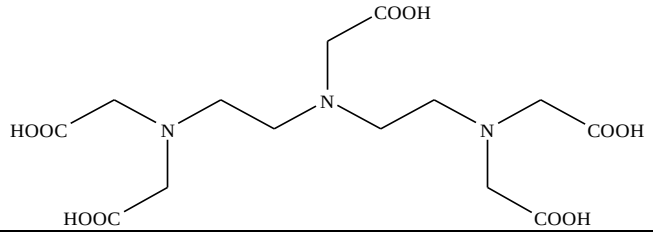

8	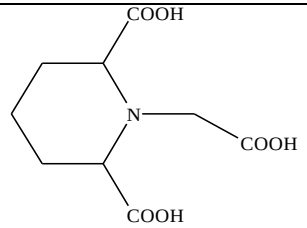
9	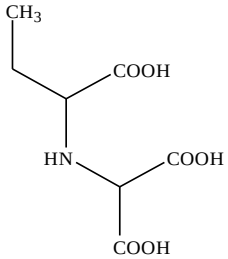
10	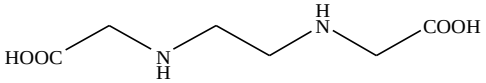
11	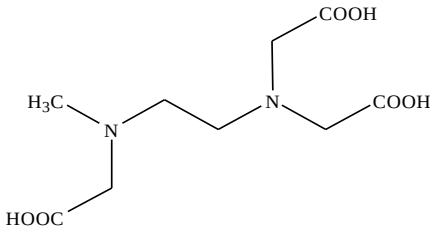
12	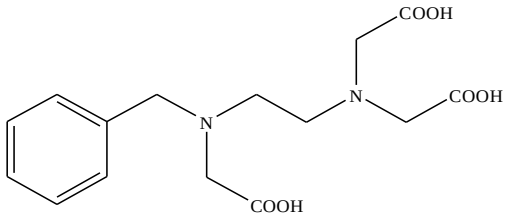
28	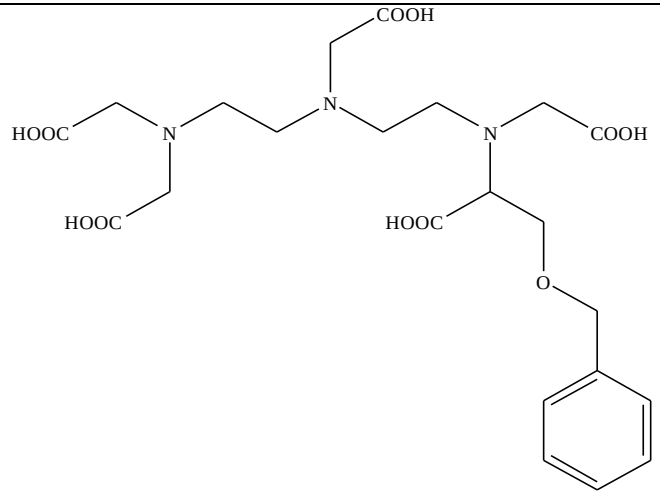
29	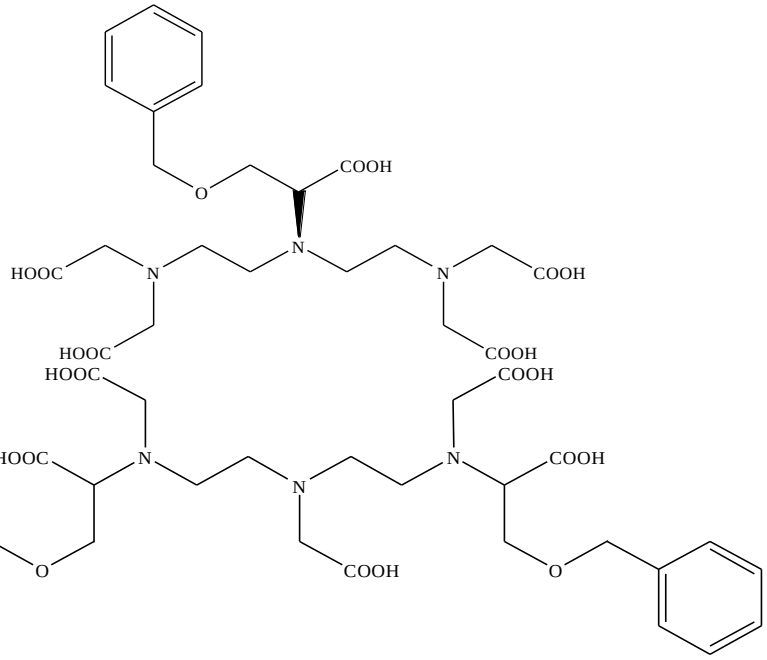
30	

13

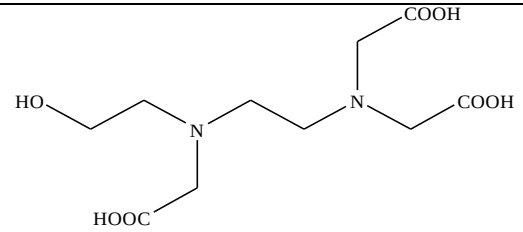

14

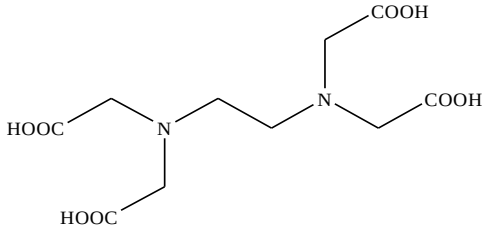

15

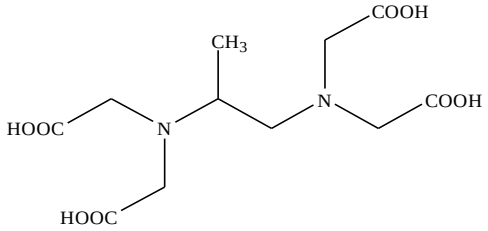

16

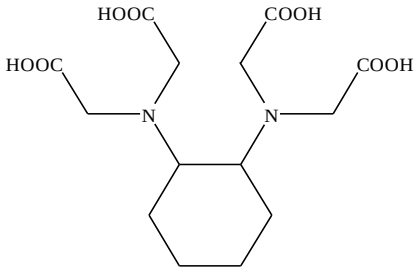

31

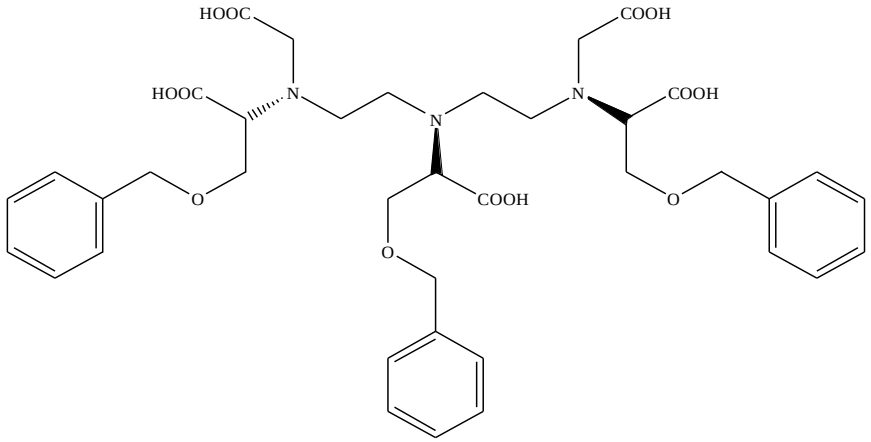

32

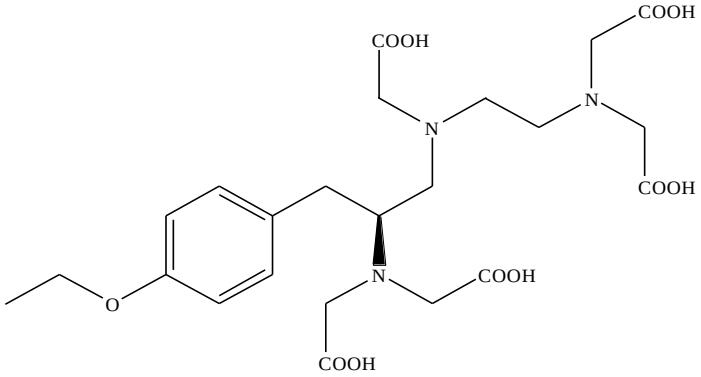

33

17

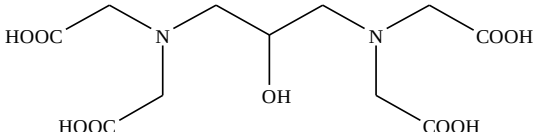
HOOC
N
N
COOH
OH
HOOC
COOH

18

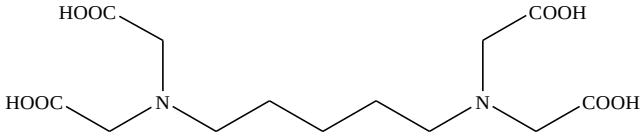
HOOC
COOH
HOOC
N
N
COOH

19

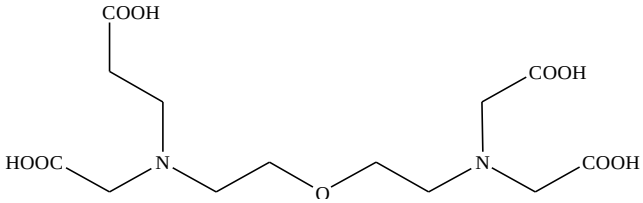
COOH
COOH
HOOC
N
N
COOH
O

20

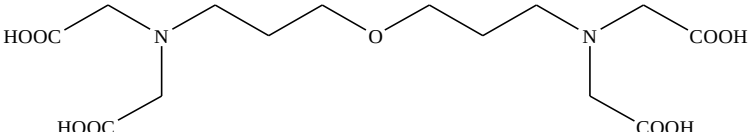
HOOC
N
O
N
COOH
HOOC
COOH

34

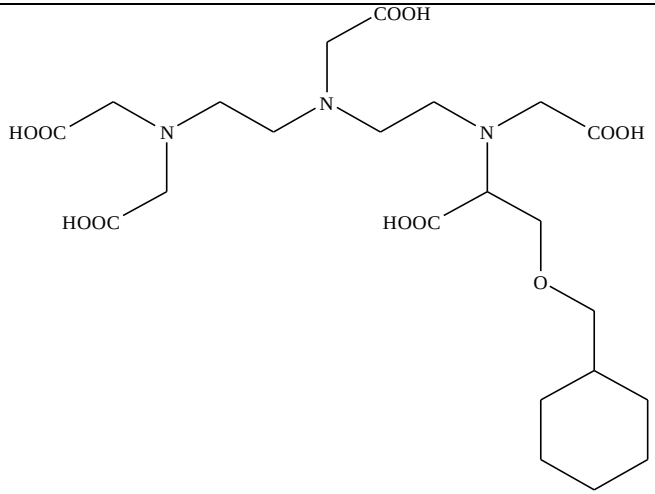
COOH
HOOC
N
N
N
COOH
HOOC
HOOC
O

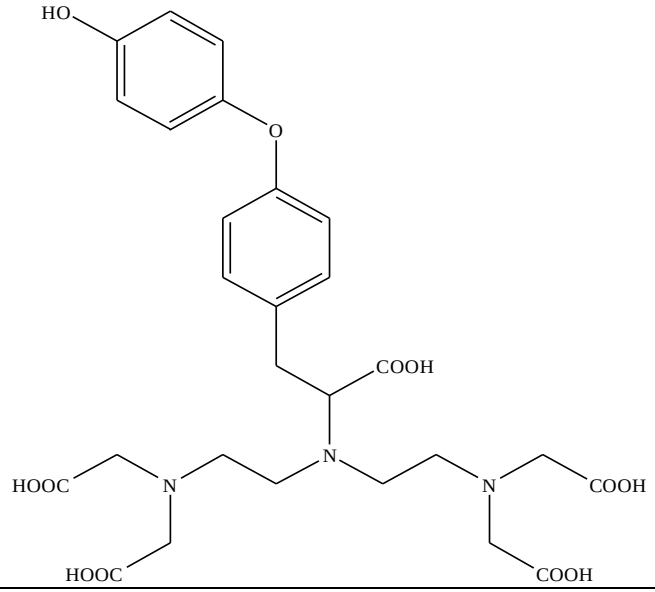
HO
O
COOH
HOOC
N
N
N
COOH
HOOC
COOH

21

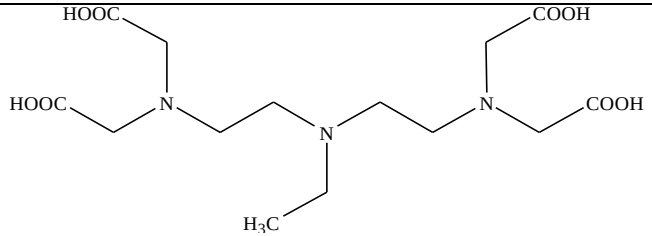

22

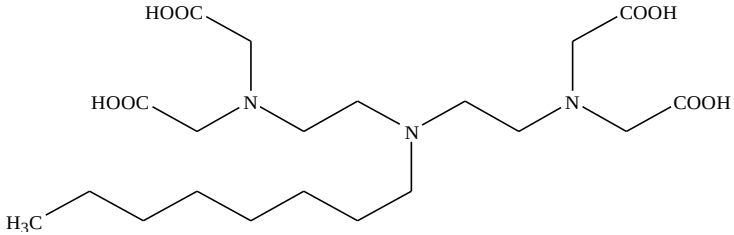

23

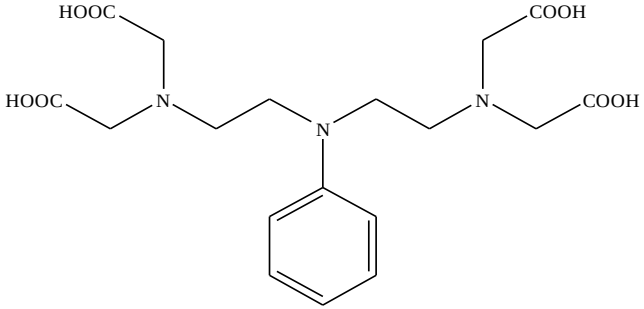

35

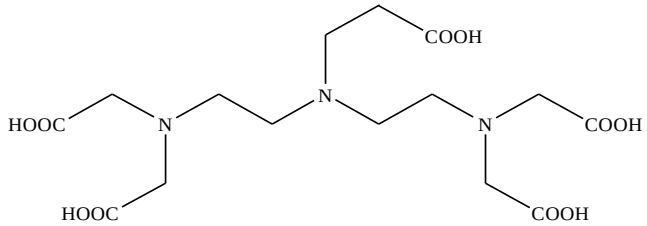

36

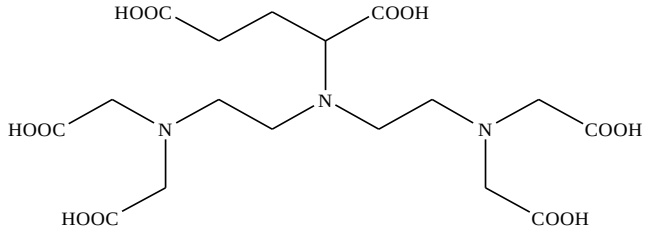

37

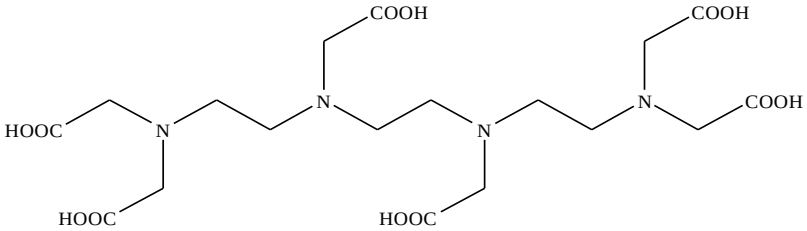

3. Results

3.1. Molecular structure

In this study, some of the electronic and molecular properties, such as the polarizability, E_{HOMO}, E_{LUMO}, the energy gap between E_{HOMO} and E_{LUMO} (ΔE), ionization energy (IE), absolute electronegativity (χ), absolute hardness (η), softness (σ), of 37 polyamino-polycarboxylic ligands for prediction of stability constants of Gd(III) complexes were calculated with the DFT/B3LYP/6-311G(d,p) and 6-311++G(2d,2p) methods for gas phase for neutral molecules, as shown in **Figures 1**-**7**.

According to the frontier molecular orbital theory (FMO), the chemical reactivity of molecule is a function of interaction between HOMO and LUMO levels of the reacting species [49]. HOMO and LUMO are known as frontier orbitals, and these energies of a molecule play important role in the determination of its molecular reactivity or stability. E_{HOMO} is associated with electron donating ability of a molecule and E_{LUMO} is associated with electron accepting ability of a molecule. High E_{HOMO} is essential for reaction with nucleophiles of molecule while low E_{LUMO} is essential for reaction with electrophiles [50]. E_{HOMO} values of the molecules being investigated were found for gas phase by using B3LYP/6-311G(d,p) and 6-311++G(2d,2p) methods. The molecules having high E_{HOMO} values tends to give electron easier and it is more prone to reaction. The electron donating trends for study molecules for gas can be written as for first five molecules: 33>30>37>28>31 with B3LYP/6-311G(d,p), and 33>37>28>31>30 with 6-311++G(2d,2p) method. E_{HOMO} values of these molecules: -5.18, -5.23, -5.38, -5.46, -5.55 eV for 6-311G(d,p) method (**Figure 1**) and -5.48, -5.61, -5.68, -5.74, -5.81 eV for 6-311++G(2d,2p) method (**Figure 2**), respectively. The molecules with the lowest E_{HOMO} values: 33<30<37<28<31 for 6-311G(d,p) method and 33<37<28<31<30 for 6-311++G(2d,2p) method can be written (see **Figures 1 and 2**).

E_{LUMO} shows that the ability of the molecule to accept electrons. Lower the value of E_{LUMO} better will be the ability to accept electrons. E_{LUMO} values of **37** molecules were found by using 6-311G(d,p) and 6-311++G(2d,2p) basic sets. The lowest E_{LUMO} values were seen at 1<15<10<18<14 for 6-311++G(2d,2p) method (**Figure 2**). Molecule **1** was found to be the easiest electron acceptor compound for 6-311G(d,p) and 6-311++G(2d,2p) methods.

HOMO-LUMO energy gap (ΔE), chemical hardness and softness are closely related to chemical properties [51-55]. Chemical hardness introduced in 1960s by Pearson [56] is defined as the resistance towards electron cloud polarization or deformation of chemical species. According to the Maximum Hardness Principle states; "a chemical system tends to arrange itself so as to achieve maximum hardness and chemical hardness can be considered as a measurement of stability" [56]. More stable molecules have large ΔE value and less stable molecules have small ΔE value. The most stable five molecules are found as 1>2>6>20>10 for 6-311G(d,p) and 1>2>6>10>4 for 6-311++G(2d,2p). The most unstable molecules are found as 31, 33 and 37 with 6-311++G(2d,2p) basic set (**Figure 3**). In general, ΔE values were found with 6-311G(d,p) to be larger than 6-311++G(2d,2p).

Ionization energy (IE) is one of the fundamental indicators of the chemical reactivity. IE (Eq. 1) can be approximated as the negative value of the E_{HOMO}. High values of the ionization energy evidence the chemical inertness and strong stability, whereas small ionization energy denotes high activity of the atoms and molecules [57]. According to ionization energy values, order of activity can be written as: 33>30>37>28>31 for 6-311G(d,p) method, and 33>37>28>31>30 for 6-311++G(2d,2p) method. Ionization energy values of these molecules were found as 5.18, 5.23, 5.38, 5.46, 5.55 eV for for 6-311G(d,p) method, and 5.48, 5.61, 5.68, 5.74, 5.81 ev for for 6-311++G(2d,2p) method, respectively. 33 molecule indicates the higher activity for both methods compared to that of other molecules. Because 33 has the lowest ionization energy value. It can be seen from **Figure 4** that the worst activitiy belongs to molecule 2.

The hardness and softness are widely used in chemistry for explaining stability of compounds. The hardness is just half the energy gap between the E_{HOMO} and E_{LUMO} (see **eq. 4**). According to Maximum Hardness Principle [58], chemical hardness is a measure of the stability of chemical species. High values of the hardness evidence strong stability as the chemical, whereas small values of hardness denote high reactivity of the atoms and molecules. Five molecules with the highest stability of chemical species are found as 1>2>6>20>10 for 6-311G(d,p) and 1>2>6>10>4 for 6-311++G(2d,2p). The first five unstable and reactivity compounds were found to be 30>28>33>37>34 for 6-311G(d,p) and 31>33>37>28>34 for 6-311++G(2d,2p).respectively. The calculated chemical hardness values are given in **Figure 5**.

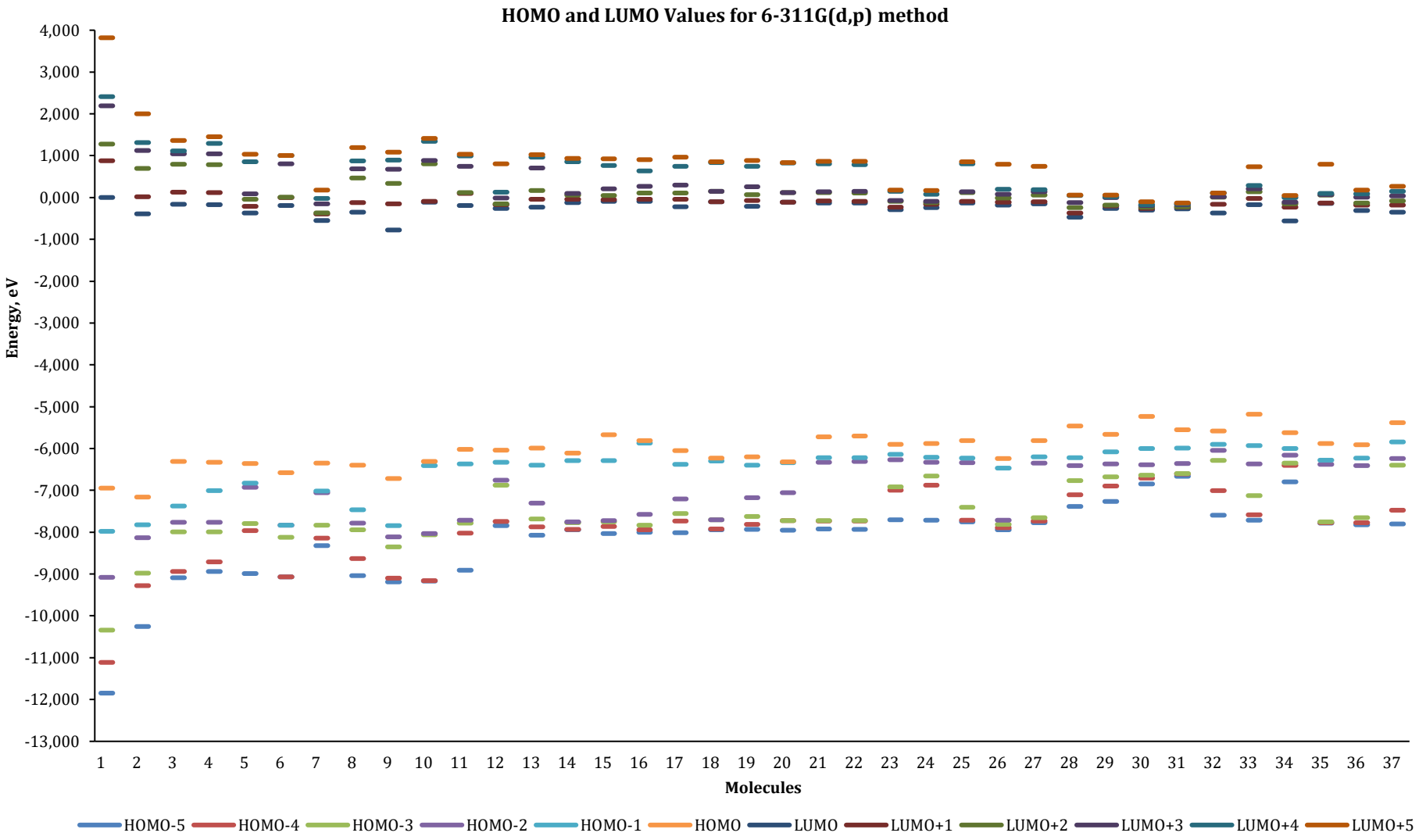

Figure 1. The calculated HOMO and LUMO parameters for the molecules under study using 6-311G(d,p) method.

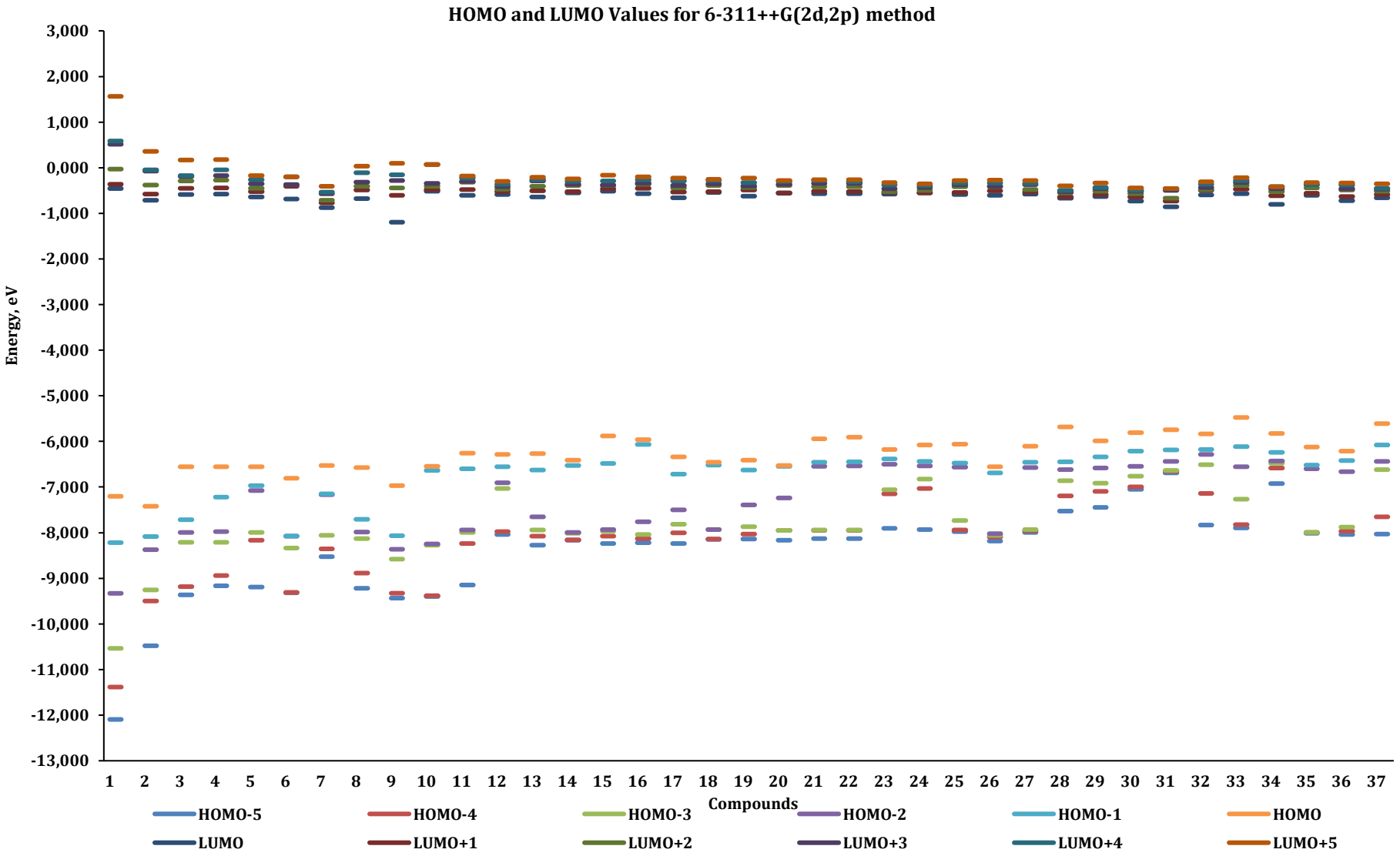

Figure 2. The calculated HOMO and LUMO parameters for the molecules under study using 6-311++G(2d,2p) method.

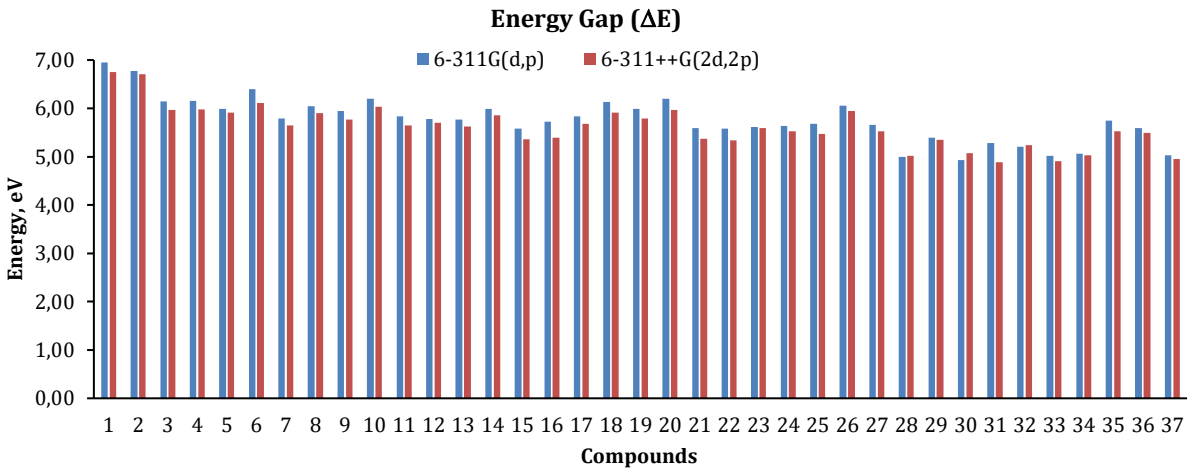

Figure 3. The calculated energy gap (ΔE) values for the molecules under study using B3LYP/6-311G(d,p) and 6-311++G(2d,2p) methods.

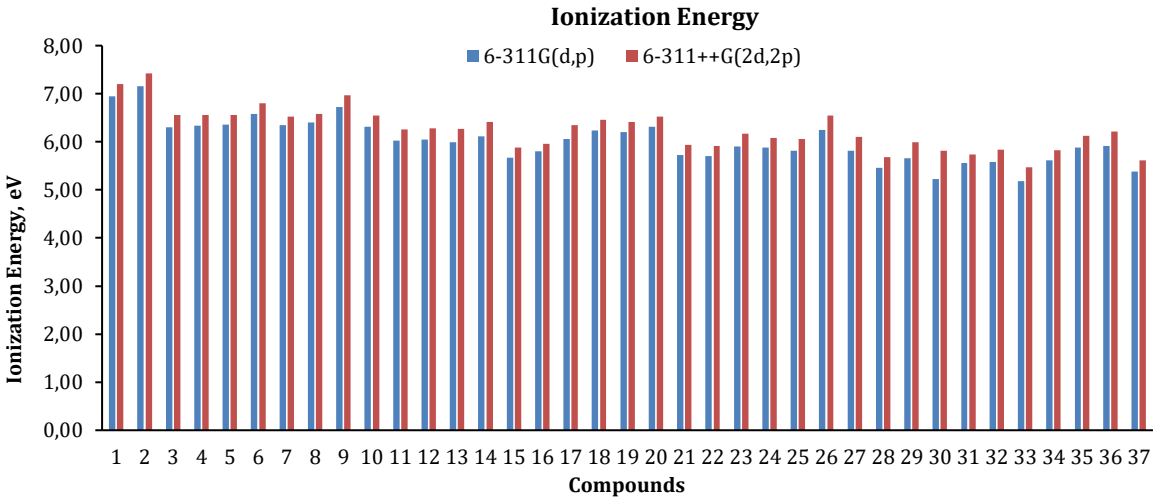

Figure 4. The ionization energy (IE) values for the molecules under study using B3LYP/6-311G(d,p) and 6-311++G(2d,2p) methods.

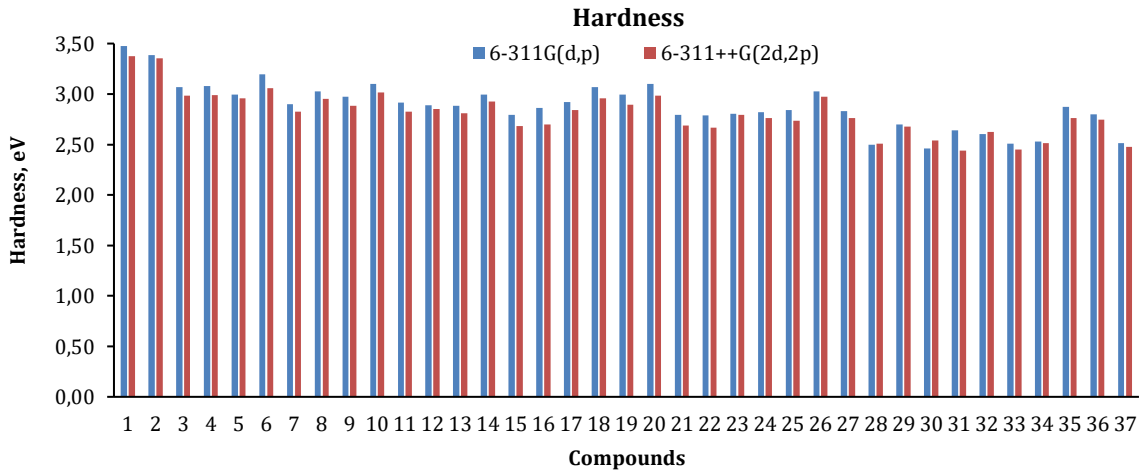

Figure 5. The calculated hardness (η) values for the molecules under study using B3LYP/6-311G(d,p) and 6-311++G(2d,2p) methods.

Softness is a measure of the polarizability and soft molecules give more easily electrons to an electron acceptor molecule [23], and they are more reactive. Low values of the softness evidence strong stability, whereas high values of softness denote high reactivity of molecules. On the basis of the calculated chemical softness values are given in **Figure 6**. According to softness values, electron donating trend of studied chemical compounds can be written as: 30>28>33>37>34 for 6-311G(d,p) and 31>33>37>28>34 for 6-311++G(2d,2p). The most difficult electron donating and unreactive molecules can be written as: 1<2<6<20<10 for 6-311G(d,p) basic set and 1<2<6<10<13 for 6-311++G(2d,2p) basic set.

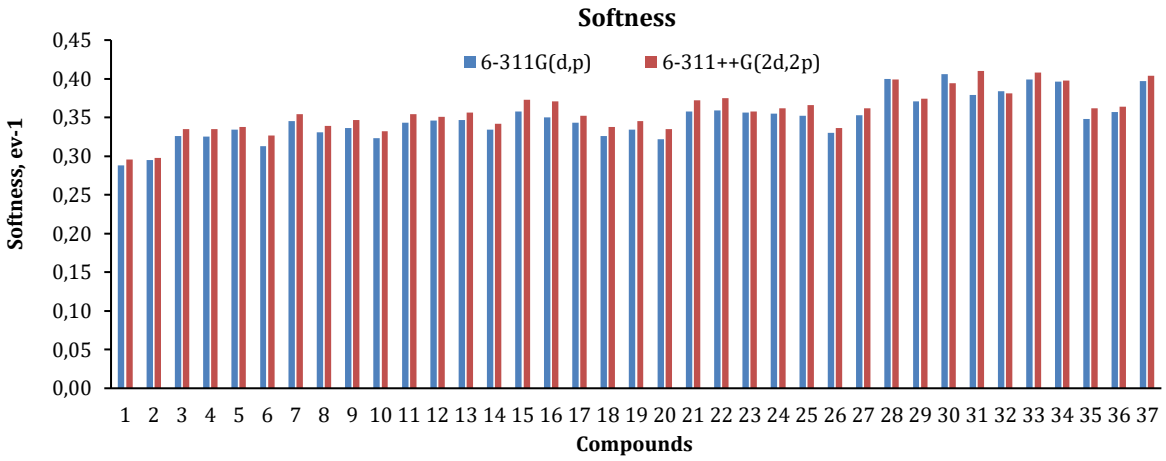

Figure 6. The calculated softness (σ) values for the molecules under study using B3LYP/6-311G(d,p) and 6-311++G(2d,2p) methods.

The average values of the HOMO and LUMO energies have been defined as the chemical potential (μ). The chemical potential was defined as the first derivative of the total energy with respect to the number of electrons. The negative of the chemical potential was known as the electronegativity (χ) (see **eq. 5**). Chemical potential, electronegativity and hardness are descriptors for the predictions about chemical properties of molecules [46]. Electronegativity that represents the power to attract the electrons of chemical species is a useful quantity in the prediction of inhibitive performance of molecules [23]. In generally, a molecule with lower electronegativity is given with easy electron donating tendency and it's known as more active [59]. The electronegativity values that can be seen in **Figure 7** were found for gas phase. According to electronegativity values, it can be seen from F**igure 7** that 33 is the most active compound than other all compounds for both basic sets.

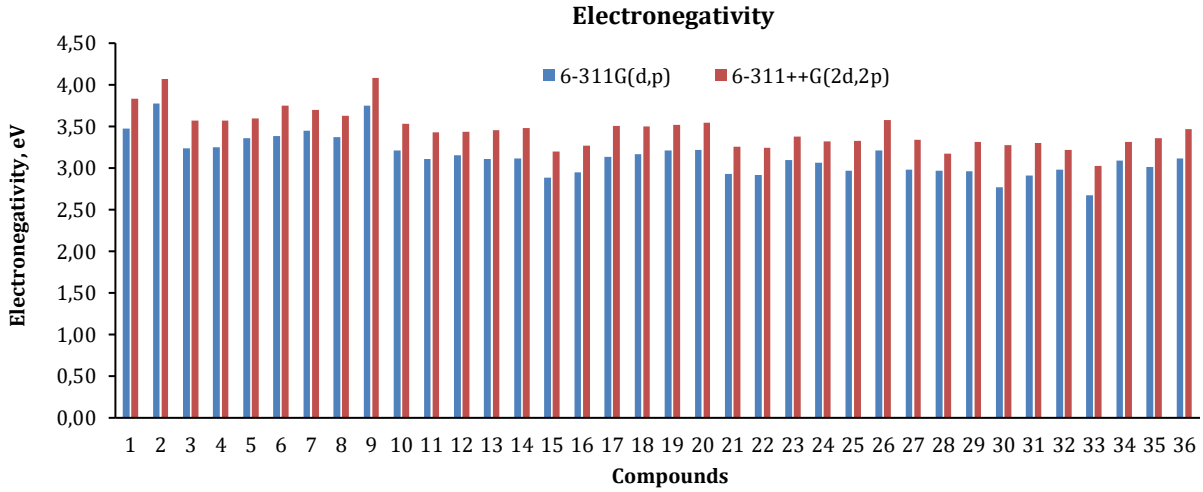

Figure 7. The calculated electronegativity (χ) values for the molecules under study using B3LYP/6-311G(d,p) and 6-311++G(2d,2p) methods.

Dipole moment (μ) is another indicator of reactivity of chemical compounds. Although some authors reported that there is no any remarkable relationship between dipole moment and reactivity [60, 53], several authors showed that increase of reactivity with the increasing of the dipole moment [53, 61]. In some studies, authors supported that increasing value of dipole moment facilitates the electron transport process [62, 63]. The calculated dipole moment values for molecules can be seen from **Tables 2** and **3**. According to dipole moment results, 34 have found to be the best active compound for both methods.

Recently, global electrophilicity (ω) have been used to by some authors as a useful information for explain the reactivity of the compounds [36, 64]. In generally, it's apparent that a good reactive compound has low electrophilicity values. 33 has found to be the best reactive compound for both methods, according to global electrophilicity results. This result can be seen from **Tables 2** and **3**.

Table 2. The calculated other quantum chemical parameter values by using B3LYP/6-311G(d,p) method.

Molecule	DM, Debye	MV, cm^3/mol	TNC, eV	μ, eV	ω, eV	SEZPE, eV
1	1.192	54.212	-1.223	-3.472	1.736	-7739.965
2	1.998	100.385	-2.060	-3.777	2.107	-13941.574
3	1.480	112.434	-2.434	-3.236	1.705	-18126.684
4	1.707	155.753	-2.497	-3.253	1.718	-19195.699
5	2.229	159.490	-2.459	-3.361	1.885	-21296.875
6	2.799	127.389	-2.659	-3.383	1.790	-20142.622
7	2.174	206.230	-3.462	-3.449	2.053	-27497.999
8	3.084	173.566	-3.381	-3.374	1.882	-24387.570
9	1.728	119.732	-2.807	-3.749	2.365	-20142.907
10	0.001	113.164	-2.478	-3.214	1.667	-17585.713
11	1.697	188.037	-3.348	-3.107	1.654	-24856.078
12	1.388	231.111	-3.771	-3.153	1.719	-31142.625
13	2.610	194.641	-3.728	-3.110	1.677	-27972.434
14	0.001	188.861	-3.965	-3.117	1.621	-29988.422
15	1.092	214.866	-3.478	-2.883	1.488	-31057.652
16	1.805	206.766	-4.731	-2.948	1.519	-34233.173
17	3.311	231.874	-4.480	-3.134	1.683	-33105.087
18	2.015	237.570	-4.561	-3.166	1.634	-33196.259
19	2.366	283.449	-4.660	-3.209	1.720	-35243.188
20	2.492	280.837	-4.778	-3.217	1.668	-36312.413
21	2.064	287.167	-4.846	-2.929	1.534	-35771.083
22	2.026	383.514	-6.074	-2.916	1.525	-42186.853
23	2.400	342.921	-4.844	-3.097	1.710	-39919.018
24	1.429	274.950	-5.070	-3.063	1.664	-40988.248
25	3.345	240.974	-5.027	-2.969	1.551	-37818.113
26	1.132	202.910	-4.667	-3.214	1.705	-35120.652
27	1.642	263.991	-4.890	-2.978	1.567	-39834.102
28	3.128	354.337	-6.250	-2.966	1.761	-50305.979
29	1.805	325.245	-6.208	-2.963	1.627	-50305.903
30	3.174	446.959	-7.332	-2.767	1.554	-60777.884
31	3.456	730.999	-6.566	-2.912	1.604	-71249.703
32	2.466	375.083	-6.568	-2.979	1.703	-51375.572
33	2.609	322.501	-6.924	-2.674	1.426	-50403.026
34	4.312	404.180	-7.017	-3.089	1.888	-57570.845
35	2.748	328.706	-5.480	-3.011	1.579	-40903.417
36	1.398	356.000	-6.377	-3.113	1.732	-47104.966
37	1.568	335.569	-6.620	-2.865	1.631	-49680.083

The sum of the total negative charge (TNC) can be seen for both methods from **Table 2** and **3**. The TNC values have been found as -7.33, -7.02, -6.92, -6.62 and -6.57 eV for 6-311G(d,p) of 30, 34, 33, 37, 32, respectively. A typical electron density distribution of total electronic charge (TNC) values calculated with the 6-311G(d,p) and 6-311++G(2d,2p) basis sets. The negative charge densities have been shown to increase on active molecules.

The results of other calculations by using 6-311G(d,p) and 6-311++G(2d,2p) basic sets, such as chemical potential (μ) values and sum of electronic and zero-point energies (SEZPE) can be seen in **Tables 2** and **3**.

Table 3. The calculated other quantum chemical parameter values by using 6-311++G(2d,2p) method.

Molecule	DM, Debye	MV, cm^3/mol	TNC, eV	μ, eV	ω, eV	SEZPE, eV
1	1.176	42.922	-1.232	-3.832	2.175	-7740.540
2	2.155	88.639	-2.062	-4.067	2.466	-13942.485
3	1.645	107.935	-3.030	-3.569	2.133	-18127.853
4	1.916	156.615	-3.158	-3.568	2.130	-19196.860
5	2.445	179.173	-4.436	-3.597	2.188	-21298.045
6	3.216	139.392	-3.813	-3.748	2.297	-20143.840
7	2.208	208.777	-4.608	-3.700	2.424	-27499.558
8	3.403	177.417	-2.000	-3.627	2.229	-24388.934
9	1.852	134.290	-3.506	-4.080	2.885	-20144.124
10	0.001	134.231	-2.664	-3.531	2.067	-17586.854
11	2.074	160.600	-4.340	-3.432	2.085	-24857.530
12	1.283	218.959	-6.315	-3.433	2.067	-31144.332
13	2.617	198.846	-4.904	-3.453	2.120	-27974.142
14	0.001	208.833	-5.413	-3.481	2.069	-29990.169
15	1.059	213.829	-5.027	-3.196	1.905	-31059.381
16	1.683	207.504	-5.200	-3.267	1.979	-34234.990
17	3.778	230.069	-6.551	-3.503	2.160	-33107.026
18	2.372	235.500	-6.146	-3.498	2.070	-33198.178
19	2.584	272.762	-5.509	-3.518	2.138	-35245.239
20	3.005	227.414	-6.652	-3.544	2.105	-36314.537
21	2.652	284.931	-6.465	-3.254	1.970	-35773.100
22	2.791	295.805	-7.558	-3.241	1.969	-42189.165
23	3.092	296.892	-6.863	-3.378	2.041	-39921.223
24	1.997	312.695	-7.918	-3.318	1.992	-40990.497
25	3.679	283.022	-6.637	-3.324	2.020	-37820.360
26	1.120	204.302	-6.447	-3.578	2.152	-35122.690
27	1.937	239.170	-7.015	-3.342	2.022	-39836.383
28	3.247	377.017	-8.859	-3.173	2.008	-50308.688
29	2.261	345.419	-9.268	-3.311	2.047	-50308.670
30	4.327	456.010	-9.027	-3.273	2.110	-60781.148
31	2.726	481.666	-10.504	-3.299	2.228	
32	2.931	451.093	-8.956	-3.216	1.972	-51378.324
33	2.138	399.106	-8.165	-3.024	1.864	-50405.701
34	4.736	493.275	-9.654	-3.314	2.184	-57573.996
35	3.195	262.465	-7.219	-3.361	2.046	-40905.767
36	3.011	253.511	-8.130	-3.465	2.188	-47107.617
37	1.560	314.521	-8.865	-3.135	1.984	-49682.795

The frontier MOs (HOMOs, LUMOs) and molecular electrostatic map (total electron density) of molecules are also given in **Figure 8**. According to the frontier molecular orbital theory (FMO), the chemical reactivity of molecule is a function of interaction between HOMO and LUMO levels of the reacting species [49]. HOMO and LUMO are known as frontier orbitals, and these a molecule play important role in the determination of its molecular reactivity or stability. Some researchers mention that Frontier orbital theory is useful in predicting the molecule's interaction center [65-67]. The electron-rich regions of the molecule can be said to be more active. The charge density distribution of HOMO and LUMO level of tetrazoles are shown in **Figure 8.**

Figure 8 shows that the electron density increases around the oxygen atoms of the all molecules. This shows us that the molecule is easier to give electrons from these regions. In such studies, electronic charge analysis for atoms in the molecules is important because binding capability of a molecule depends also on electronic charge of the molecules. The binding facilitates as the negative charge on atoms increases [68].

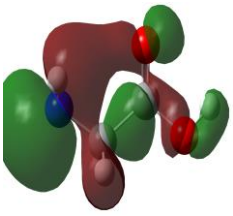
1-HOMO

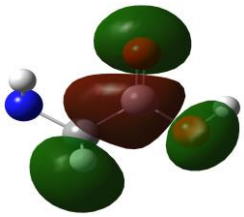
1-LUMO

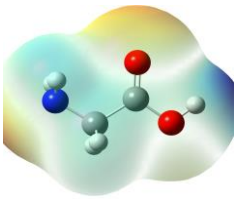
1-Total Density

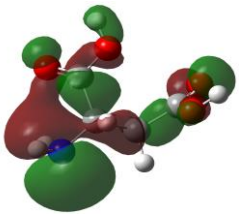
2-HOMO

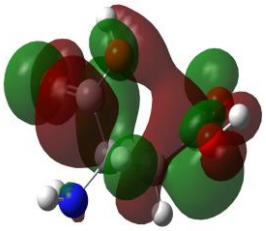
2-LUMO

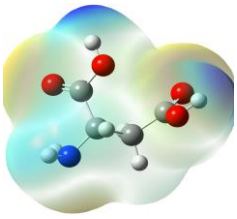
2-Total Density

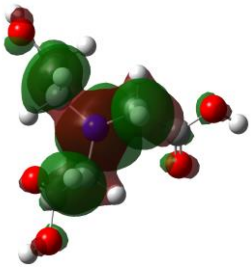
3-HOMO

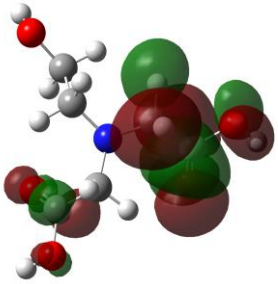
3-LUMO

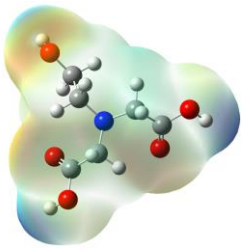
3-Total Density

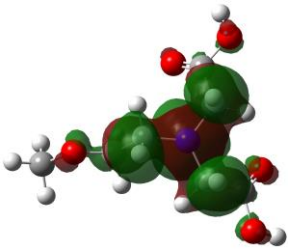
4-HOMO

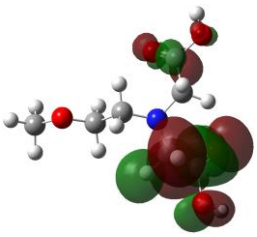
4-LUMO

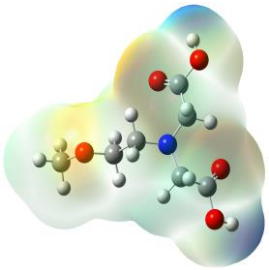
4-Total Density

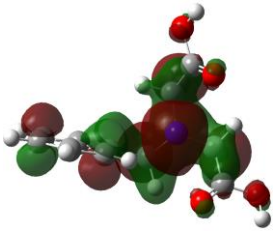
5-HOMO

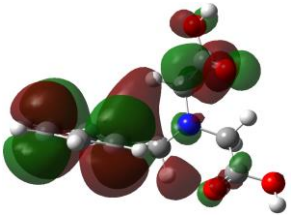
5-LUMO

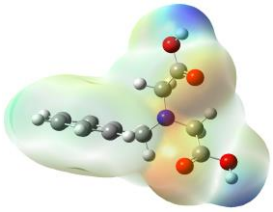
5-Total Density

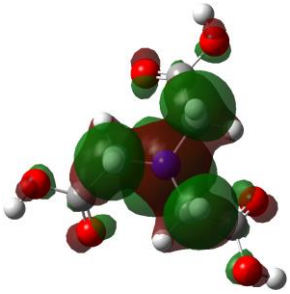
6-HOMO

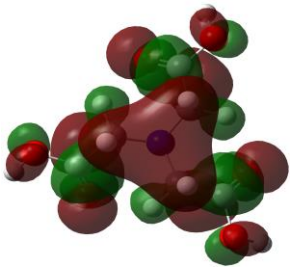
6-LUMO

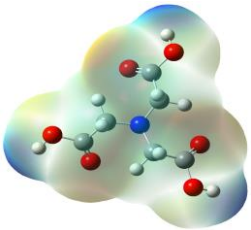
6-Total Density

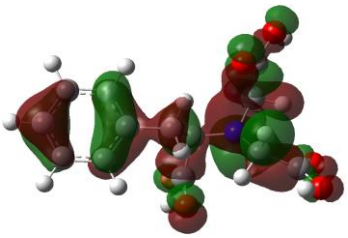

7-HOMO

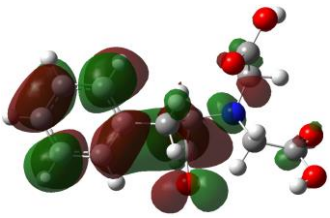

7-LUMO

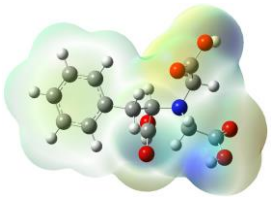

7-Total Density

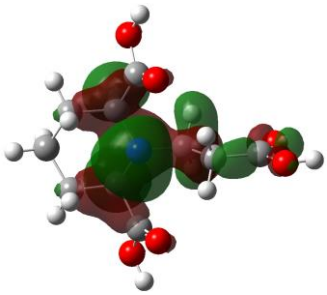

8-HOMO

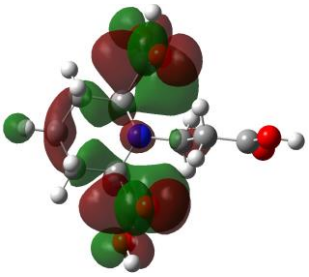

8-LUMO

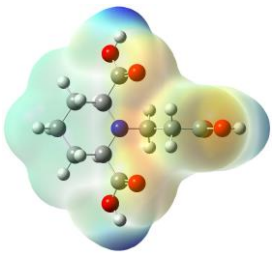

8-Total Density

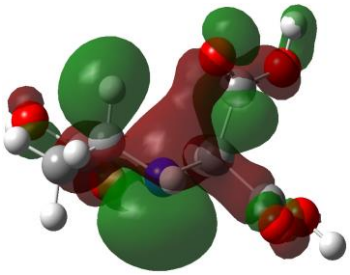

9-HOMO

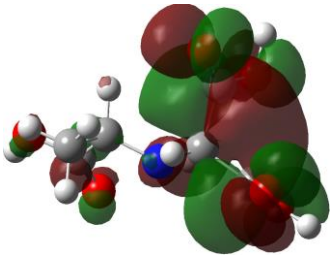

9-LUMO

9-Total Density

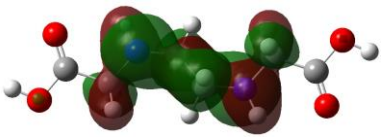

10-HOMO

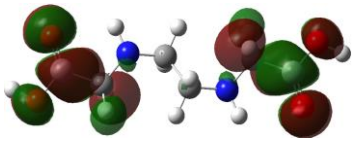

10-LUMO

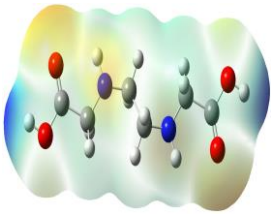

10-Total Density

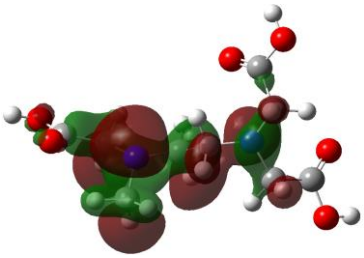

11-HOMO

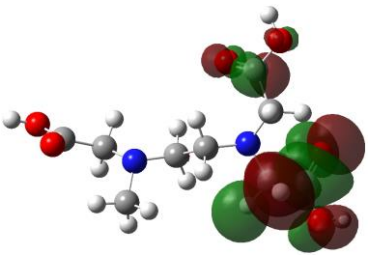

11-LUMO

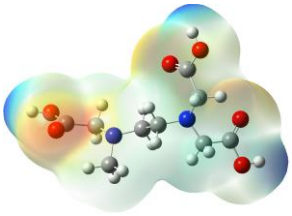

11-Total Density

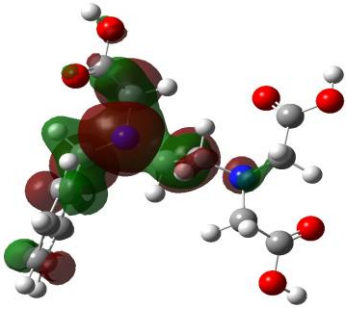

12-HOMO

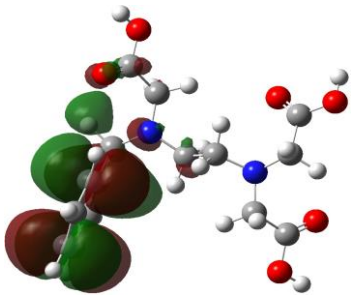

12-LUMO

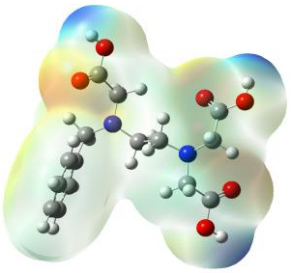

12-Total Density

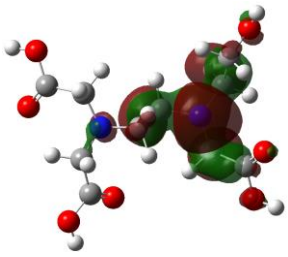

13-HOMO

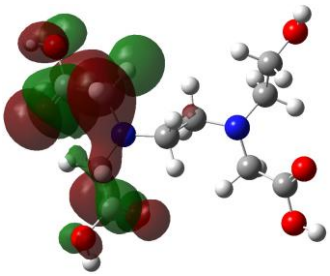

13-LUMO

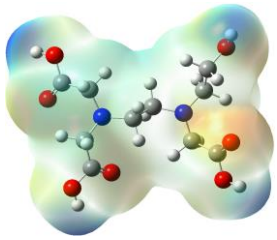

13-Total Density

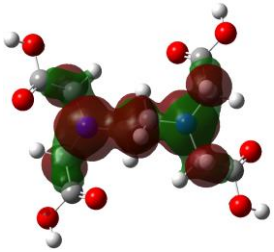

14-HOMO

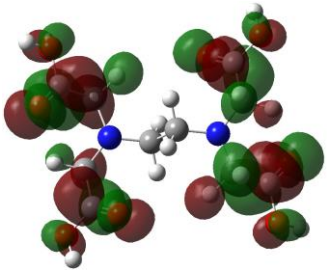

14-LUMO

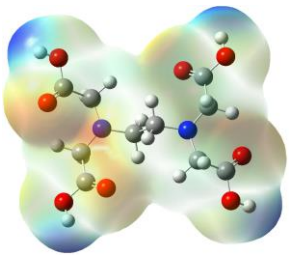

14-Total Density

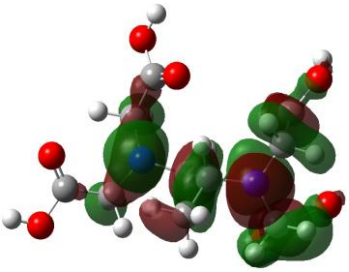

15-HOMO

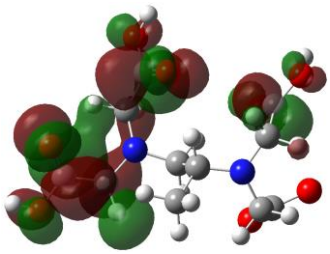

15-LUMO

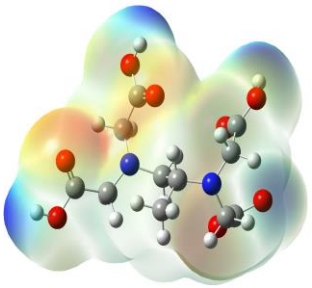

15-Total Density

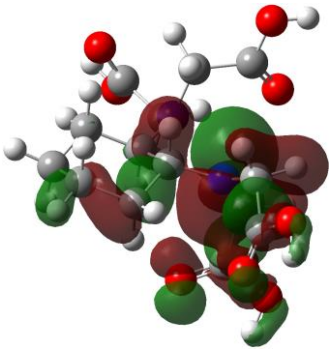

16-HOMO

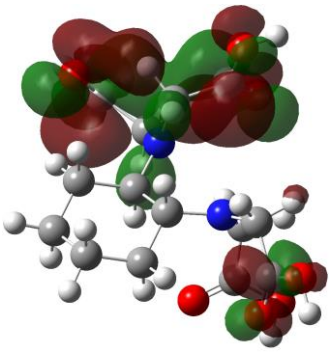

16-LUMO

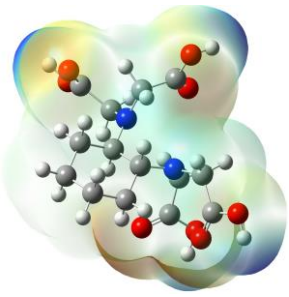

16-Total Density

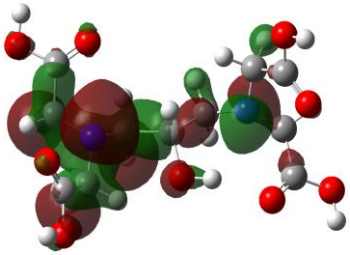

17-HOMO

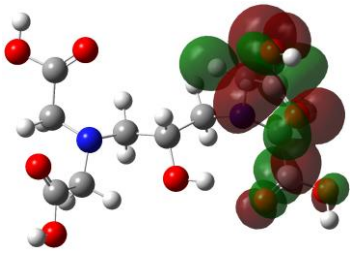

17-LUMO

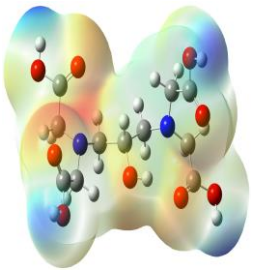

17-Total Density

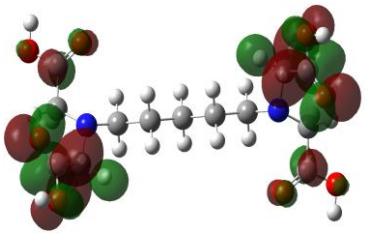

18-HOMO

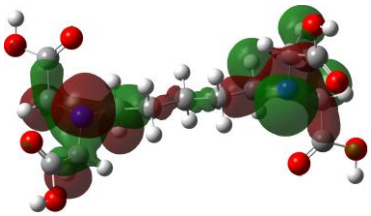

18-LUMO

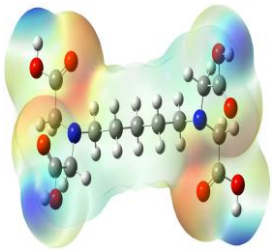

18-Total Density

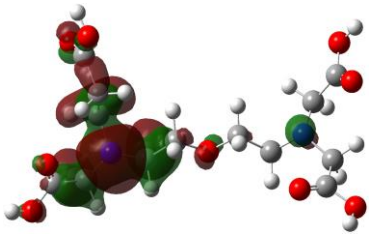

19-HOMO

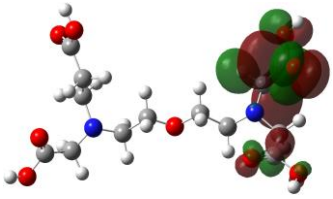

19-LUMO

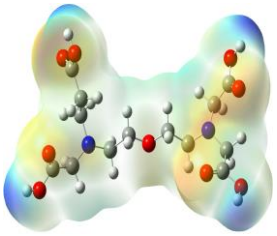

19-Total Density

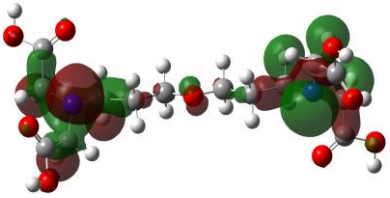

20-HOMO

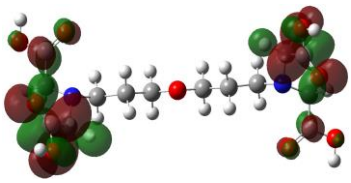

20-LUMO

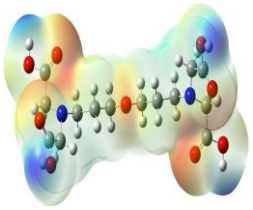

20-Total Density

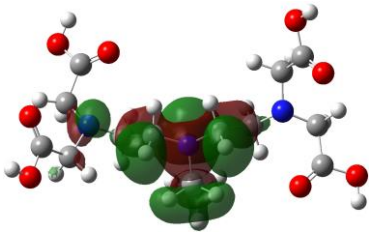

21-HOMO

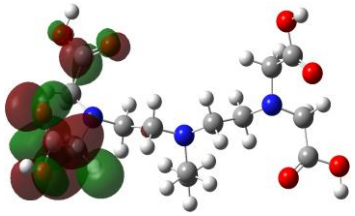

21-LUMO

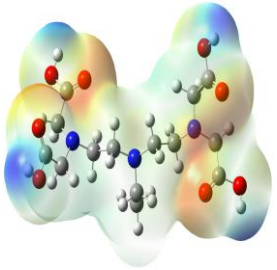

21-Total Density

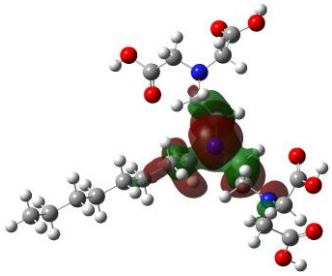

22-HOMO

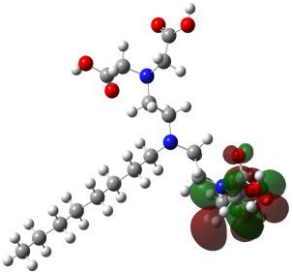

22-LUMO

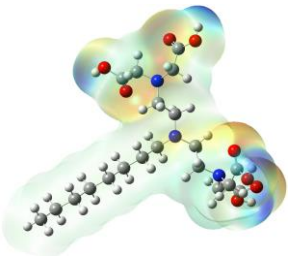

22-Total Density

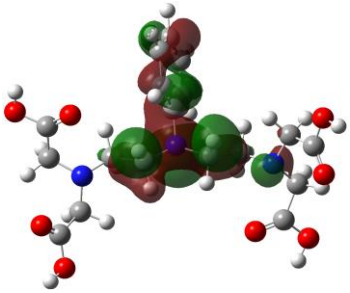

23-HOMO

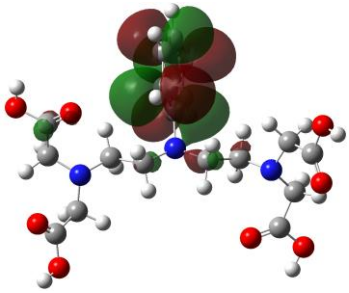

23-LUMO

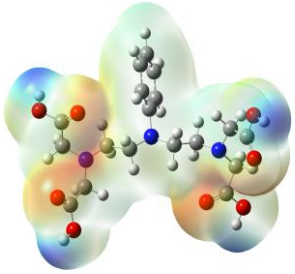

23-Total Density

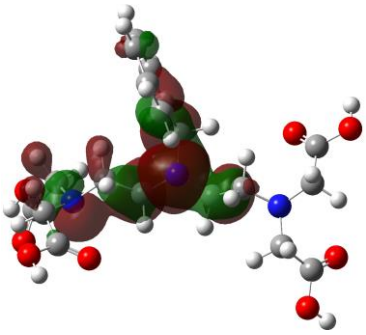

24-HOMO

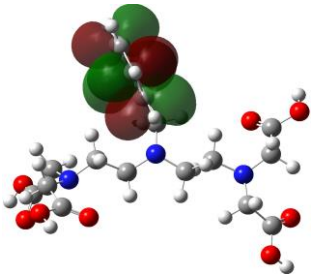

24-LUMO

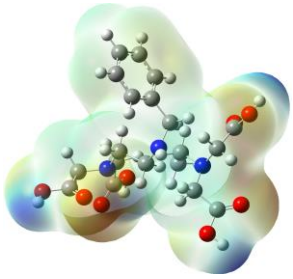

24-Total Density

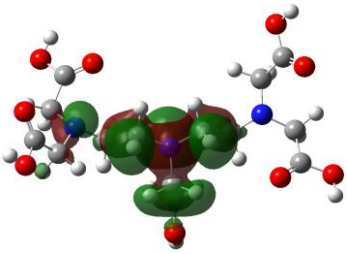

25-HOMO

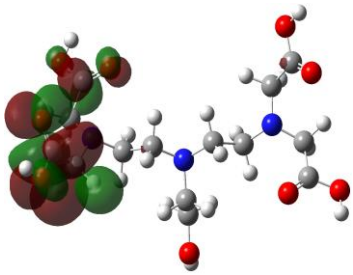

25-LUMO

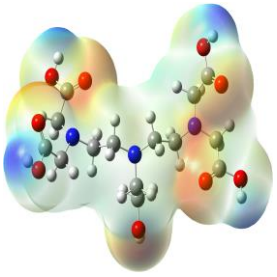

25-Total Density

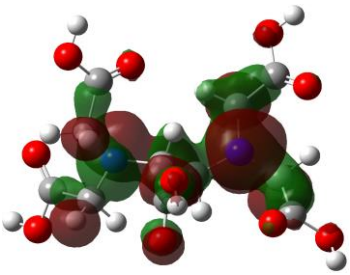

26-HOMO

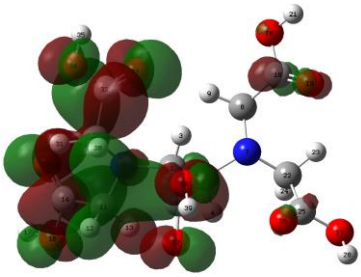

26-LUMO

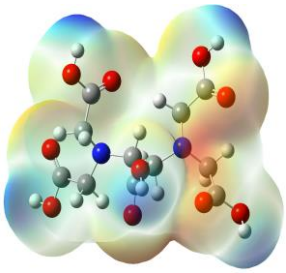

26-Total Density

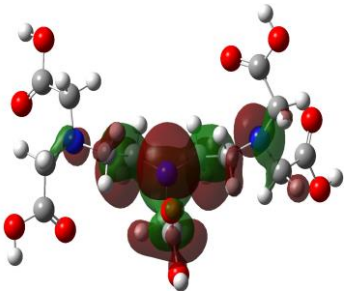

27-HOMO

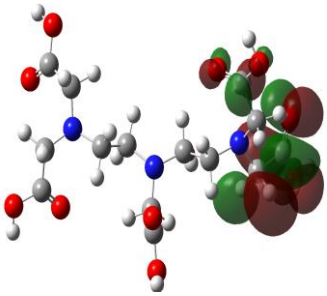

27-LUMO

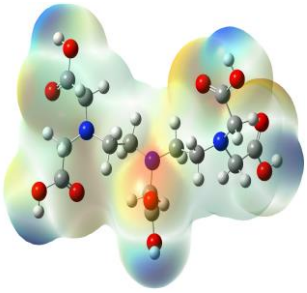

27-Total Density

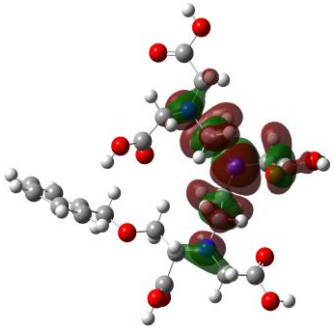

28-HOMO

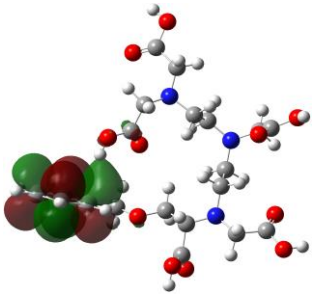

28-LUMO

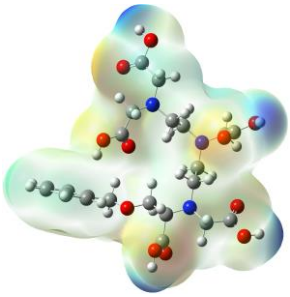

28-Total Density

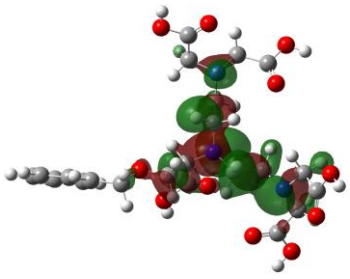

29-HOMO

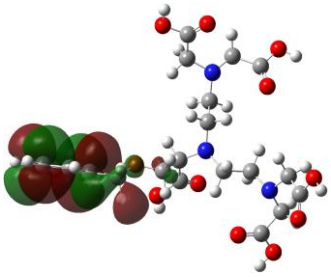

29-LUMO

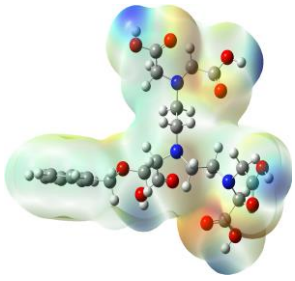

29-Total Density

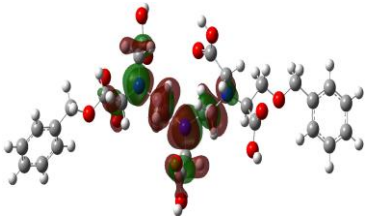

30-HOMO

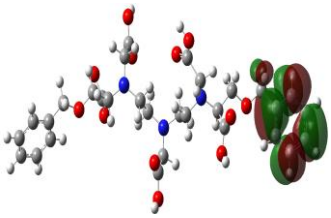

30-LUMO

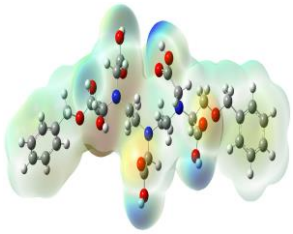

30-Total Density

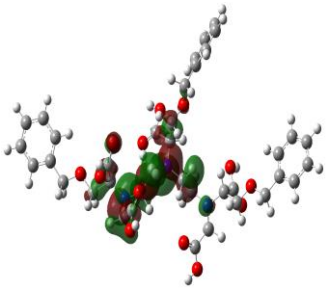

31-HOMO

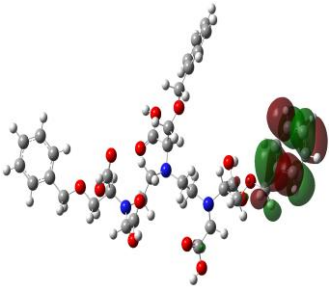

31-LUMO

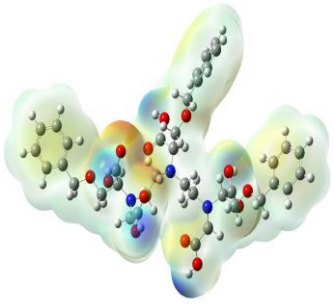

31-Total Density

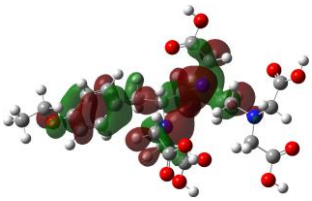

32-HOMO

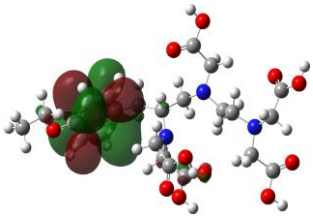

32-LUMO

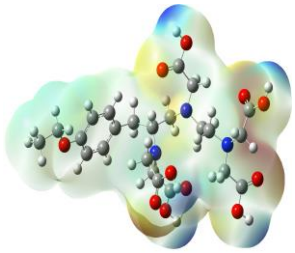

32-Total Density

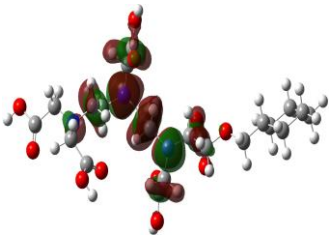

33-HOMO

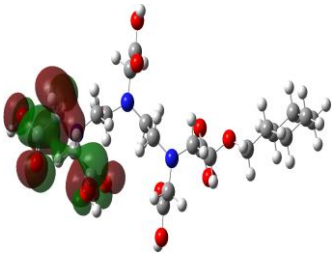

33-LUMO

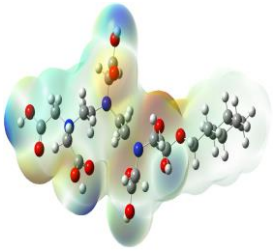

33-Total Density

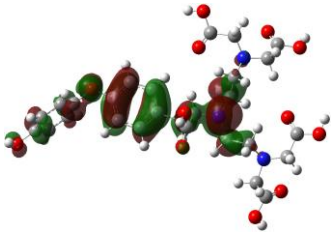

34-HOMO

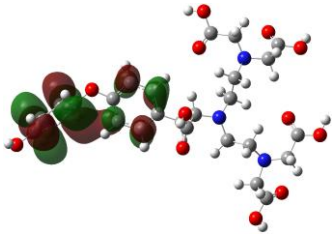

34-LUMO

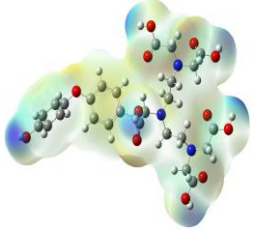

34-Total Density

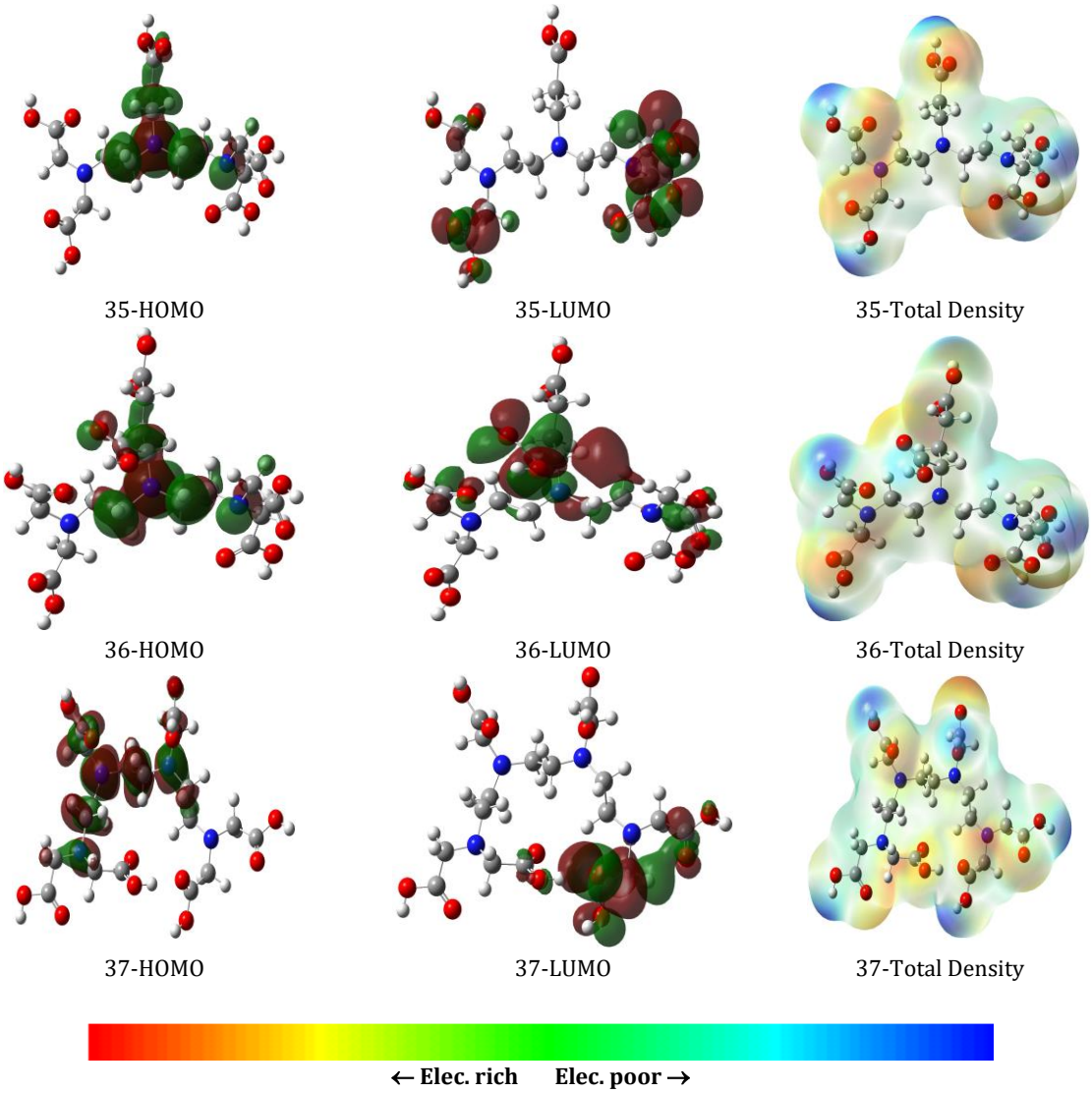

Figure 8. The frontier MOs (HOMOs, LUMOs) and molecular electrostatic map (total electron density) of molecules by using DFT/B3LYP/6-311++G(2d,2p) basic set.

The HOMO and LUMO orbitals contribution of the atoms for all molecules are shown in **Tables 4** and **5**. The HOMO and LUMO orbitals were calculated with AOmix program [20, 21] after optimization with DFT/B3LYP/6-311G(d,p) method for gas phase. It can be seen from **Table 4** that the HOMO orbitals of all molecules are composed mainly of **N** atoms. Similarly, the LUMO orbitals of all molecules are composed mainly of **C** atoms (see **Table 5**). For more details on HOMO and LUMO values, see supplementary Table S1.

3.2. Statistical Analysis

Twelve descriptors, namely, E_{HOMO}, E_{LUMO}, ΔE, DM, MV, TNC, η, σ, χ, μ, ω and SEZPE whose values were calculated by B3LYP/6-311G(d,p) method for 37 molecules was employed to construct a model between those variables and log K values. Factor analysis was conducted in order to determine the co-linearity among descriptor variables and to obtain the sets of descriptors that are statistically independent of each other. The descriptors pertinent to each factor with factor loadings are bold and summarized in **Table 6**. Therefore, while first factor consists of E_{HOMO}, ΔE, DM, MV, η, σ, χ, μ and SEZPE, the second factor composes of E_{LUMO} and ω. The total variance explained by two factors is 88.90.

Table 4. Represents the highest occupied molecular orbital (HOMO) population for the molecules under study by using AOMIX program after from B3LYP/6-311G(d,p) method.

Molecule	Calculated HOMO by using Aomix method
1	+ 19.6% 4PX(N3) + 15.9% 3PX(N3) + 11.4% 3PY(N3) + 10.4% 4PY(N3) + 8.0% 2PX(N3) + 5.7% 2PY(N3)
2	+ 23.1% 4PY(N5) + 20.3% 3PY(N5) + 10.2% 2PY(N5) - 5.6% 3PX(N5) - 4.5% 4PX(N5) - 3.5% 3S(N5)
3	+ 27.3% 3PZ(N6) + 21.7% 4PZ(N6) + 13.7% 2PZ(N6) - 3.2% 4S(N6) - 2.4% 2S(H15) - 2.4% 2S(H17)
4	+ 27.1% 3PZ(N6) + 21.5% 4PZ(N6) + 13.7% 2PZ(N6) - 3.2% 4S(N6) - 2.4% 2S(H19) - 2.4% 2S(H17)
5	+ 22.7% 3PZ(N5) + 17.8% 4PZ(N5) + 11.4% 2PZ(N5) + 3.1% 4S(N5) + 2.5% 2S(H18) + 2.1% 2S(H22)
6	+ 27.1% 3PZ(N7) + 21.3% 4PZ(N7) + 13.6% 2PZ(N7) - 3.2% 4S(N7) - 2.5% 2S(H15) - 2.5% 2S(H19)
7	- 10.2% 3PZ(N7) + 8.5% 3PY(N7) + 8.4% 4PY(N7) - 7.3% 4PZ(N7) - 5.1% 2PZ(N7) + 4.4% 2PY(N7)
8	+ 26.6% 3PZ(N23) + 21.5% 4PZ(N23) + 13.4% 2PZ(N23) - 3.2% 4S(N23) - 2.4% 2S(H13) - 2.4% 2S(H15)
9	+ 24.8% 3PY(N1) + 22.8% 4PY(N1) + 12.4% 2PY(N1) - 3.1% 4S(N1) - 3.0% 2S(H14) - 1.9% 3S(N1)
10	+ 12.5% 3PZ(N7) - 12.5% 3PZ(N9) + 11.5% 4PZ(N7) - 11.5% 4PZ(N9) + 6.4% 2PZ(N7) - 6.4% 2PZ(N9)
11	+ 12.6% 3PY(N7) + 10.6% 4PY(N7) + 10.3% 3PZ(N7) + 7.6% 4PZ(N7) + 6.4% 2PY(N7) + 5.2% 2PZ(N7)
12	+ 23.8% 3PZ(N7) + 18.9% 4PZ(N7) + 12.0% 2PZ(N7) + 3.3% 4S(N7) + 2.4% 2S(H31) + 2.0% 2S(H4)
13	+ 26.6% 3PZ(N7) + 21.3% 4PZ(N7) + 13.4% 2PZ(N7) + 3.3% 4S(N7) + 2.1% 2S(H13) + 2.1% 2S(H4)
14	+ 13.0% 3PZ(N7) - 12.9% 3PZ(N8) + 10.3% 4PZ(N7) - 10.3% 4PZ(N8) + 6.6% 2PZ(N7) - 6.5% 2PZ(N8)
15	+ 17.6% 3PZ(N6) + 14.3% 4PZ(N6) + 9.0% 2PZ(N6) - 6.4% 3PZ(N7) - 4.8% 4PZ(N7) - 3.3% 2PZ(N7)
16	+ 11.5% 3PX(N17) + 11.4% 3PY(N17) + 10.1% 4PX(N17) + 9.1% 4PY(N17) + 5.9% 2PX(N17) + 5.8% 2PY(N17)
17	+ 18.4% 3PZ(N6) + 14.5% 4PZ(N6) + 9.3% 2PZ(N6) + 3.8% 3PY(N6) + 3.1% 4PY(N6) + 3.0% 4S(N6)
18	+ 8.4% 3PZ(N6) - 8.4% 3PZ(N31) + 6.7% 4PZ(N6) - 6.7% 4PZ(N31) + 4.5% 3PY(N6) + 4.5% 3PY(N31)
19	+ 25.5% 3PZ(N28) + 20.3% 4PZ(N28) + 12.8% 2PZ(N28) + 2.8% 4S(N28) + 2.6% 2S(H25) + 2.4% 2S(H31)
20	+ 6.9% 3PZ(N35) - 6.9% 3PZ(N6) + 5.9% 3PY(N35) + 5.9% 3PY(N6) + 5.6% 4PZ(N35) - 5.6% 4PZ(N6)
21	+ 22.0% 3PZ(N43) + 18.1% 4PZ(N43) + 11.1% 2PZ(N43) - 4.0% 3PY(N43) - 3.2% 4S(N43) - 2.8% 4PY(N43)
22	+ 25.1% 3PZ(N43) + 19.9% 4PZ(N43) + 12.6% 2PZ(N43) + 3.2% 4S(N43) + 2.5% 2S(H24) + 2.4% 2S(H3)
23	+ 20.3% 3PZ(N43) + 16.8% 4PZ(N43) + 10.3% 2PZ(N43) + 3.7% 3PY(N43) + 3.0% 4PY(N43) - 2.7% 2S(H3)
24	+ 21.7% 3PZ(N43) + 17.1% 4PZ(N43) + 10.9% 2PZ(N43) + 2.9% 4S(N43) - 2.5% 3PY(N28) + 2.3% 2S(H24)
25	+ 23.0% 3PZ(N43) + 19.0% 4PZ(N43) + 11.6% 2PZ(N43) - 3.1% 4S(N43) - 2.5% 2S(H24) - 2.5% 2S(H3)
26	+ 18.1% 3PZ(N7) + 14.2% 4PZ(N7) + 9.1% 2PZ(N7) - 5.0% 3PZ(N6) - 4.1% 4PZ(N6) - 2.6% 2PZ(N6)
27	+ 23.8% 3PZ(N43) + 18.8% 4PZ(N43) + 12.0% 2PZ(N43) + 2.5% 4S(N43) + 2.4% 2S(H24) + 2.3% 2S(H3)
28	+ 23.2% 3PZ(N42) + 18.3% 4PZ(N42) + 11.7% 2PZ(N42) + 2.0% 3PZ(C21) - 1.9% 3PZ(N27) + 1.8% 3PZ(C2)
29	+ 17.9% 3PZ(N43) + 13.9% 4PZ(N43) + 9.0% 2PZ(N43) - 3.7% 3PX(N43) - 3.3% 4PX(N43) - 1.9% 2PX(N43)
30	+ 18.6% 3PZ(N41) + 14.6% 4PZ(N41) + 9.4% 2PZ(N41) - 6.6% 3PZ(N6) - 5.2% 4PZ(N6) - 3.4% 2PZ(N6)
31	+ 10.0% 3PZ(N41) + 8.1% 4PZ(N41) - 5.5% 3PZ(N6) + 5.1% 2PZ(N41) - 4.5% 4PZ(N6) - 4.1% 3PY(N6)
32	+ 12.4% 3PZ(N22) + 9.9% 4PZ(N22) + 6.3% 2PZ(N22) + 4.7% 3PX(N56) + 4.0% 4PX(N56) - 3.2% 3PX(N22)
33	+ 18.0% 3PZ(N42) + 14.0% 4PZ(N42) + 9.1% 2PZ(N42) - 8.0% 3PZ(N6) - 6.4% 4PZ(N6) - 4.1% 2PZ(N6)
34	+ 10.9% 3PZ(N42) + 9.0% 4PZ(N42) + 5.5% 2PZ(N42) - 4.2% 3PZ(C53) - 3.8% 3PZ(O61) + 3.7% 3PZ(C60)
35	+ 25.0% 3PZ(N43) + 20.2% 4PZ(N43) + 12.6% 2PZ(N43) - 3.1% 4S(N43) - 2.5% 2S(H24) - 2.4% 2S(H3)
36	+ 23.7% 3PZ(N43) + 19.4% 4PZ(N43) + 12.0% 2PZ(N43) - 2.7% 2S(H3) - 2.7% 4S(N43) - 2.1% 2S(H24)
37	+ 19.5% 3PZ(N6) + 15.3% 4PZ(N6) + 9.9% 2PZ(N6) - 4.7% 3PZ(N36) - 3.7% 4PZ(N36) - 2.4% 2PZ(N36)

Table 5. Represents the highest occupied molecular orbital (LUMO) population for molecules by using Aomix method after from B3LYP/6-311G(d,p) method.

Molecule	Calculated LUMO by using Aomix method
1	+ 24.7% 3PZ(C5) + 15.7% 4PZ(C5) + 12.9% 2PZ(C5) - 11.1% 3PZ(O2) - 7.0% 2PZ(O2) - 6.9% 4PZ(O2)
2	+ 12.6% 3PZ(C8) + 7.2% 4PZ(C8) + 6.5% 2PZ(C8) - 6.0% 3PZ(O3) - 5.2% 3PX(C8) + 3.8% 3PY(C9)
3	- 13.4% 3PZ(C12) + 8.3% 3PY(C12) - 7.5% 4PZ(C12) - 7.0% 2PZ(C12) + 6.2% 3PZ(O5) + 5.9% 4PY(C12)
4	- 11.5% 3PZ(C11) - 9.5% 3PX(C11) - 6.3% 4PZ(C11) - 6.1% 4PX(C11) - 6.0% 2PZ(C11) + 5.3% 3PZ(O4)
5	+ 8.6% 4PY(C16) - 8.0% 4PY(C10) + 7.0% 3PY(C16) - 6.7% 4PY(C15) + 6.7% 3PY(C7) + 6.6% 4PY(C7)
6	+ 4.4% 3S(H19) + 4.3% 3S(H15) + 4.3% 3S(H17) - 4.2% 3PZ(C13) - 4.1% 3PZ(C11) - 4.0% 3PZ(C12)
7	- 8.7% 3PX(C13) + 6.9% 4PZ(C15) - 6.3% 4PX(C13) + 6.2% 4PZ(C18) + 5.5% 3PZ(C18) + 5.5% 3PZ(C15)
8	+ 7.1% 3PX(C25) + 7.1% 3PX(C29) + 4.7% 4PX(C25) + 4.7% 4PX(C29) - 4.1% 3PZ(C25) - 4.1% 3PZ(C29)
9	+ 8.5% 3PX(C9) + 7.3% 4PX(C9) + 5.6% 3PX(C5) + 4.6% 3PY(C5) + 4.5% 3PZ(C9) + 4.3% 2PX(C9)
10	+ 12.3% 3PZ(C21) - 12.2% 3PZ(C17) + 7.4% 4PZ(C21) - 7.3% 4PZ(C17) + 6.4% 2PZ(C21) - 6.4% 2PZ(C17)
11	- 11.6% 3PZ(C19) - 9.4% 3PX(C19) - 6.5% 4PZ(C19) - 6.1% 2PZ(C19) - 6.0% 4PX(C19) + 5.4% 3PZ(O20)
12	+ 9.6% 4PX(C35) + 8.7% 4PX(C36) - 8.4% 4PX(C40) + 7.3% 3PX(C35) + 7.0% 3PX(C36) - 6.7% 3PX(C40)
13	- 12.6% 3PZ(C19) - 7.1% 4PZ(C19) + 6.6% 3PX(C19) - 6.6% 2PZ(C19) + 5.9% 3PZ(O20) + 4.6% 3S(H11)
14	+ 4.2% 3PZ(C19) + 4.1% 3PZ(C15) + 2.7% 3PX(C19) + 2.6% 3PX(C15) + 2.5% 3PZ(C26) + 2.4% 3PZ(C33)
15	+ 11.2% 3PZ(C18) + 6.8% 4PZ(C18) + 5.9% 2PZ(C18) - 5.6% 3PZ(O19) - 3.5% 3PX(C25) - 3.5% 2PZ(O19)
16	+ 13.6% 3PY(C43) + 8.6% 4PY(C43) + 7.4% 3PX(C29) + 7.1% 2PY(C43) - 5.5% 3PY(O44) + 4.9% 4PX(C29)
17	- 12.5% 3PX(C31) - 8.3% 4PX(C31) - 6.5% 2PX(C31) + 5.6% 3PX(O32) + 4.9% 3PZ(C31) + 4.3% 3S(H27)
18	- 6.6% 3PX(C42) + 6.4% 3PX(C10) - 4.2% 4PX(C42) + 4.1% 4PX(C10) + 3.7% 3PZ(C42) + 3.6% 3PZ(C10)
19	- 14.6% 3PX(C10) - 9.4% 4PX(C10) - 7.7% 2PX(C10) + 6.5% 3PX(O11) + 5.5% 3PZ(C10) + 4.9% 3S(H9)
20	+ 8.9% 3PX(C46) + 5.8% 4PX(C46) - 4.8% 3PX(C10) + 4.7% 2PX(C46) - 3.9% 3PX(O47) + 3.4% 3PZ(C46)
21	+ 13.6% 3PX(C39) + 8.5% 4PX(C39) + 8.1% 3PZ(C39) + 7.1% 2PX(C39) - 6.0% 3PX(O40) + 5.1% 4PZ(C39)
22	+ 18.0% 3PY(C39) + 10.5% 4PY(C39) + 9.4% 2PY(C39) - 8.2% 3PY(O40) - 5.2% 4PY(O40) - 5.1% 2PY(O40)
23	+ 12.4% 4PX(C46) + 12.1% 4PX(C47) + 9.9% 3PX(C47) + 9.5% 3PX(C46) + 5.5% 2PX(C47) + 5.3% 2PX(C46)
24	+ 11.2% 4PX(C48) + 10.2% 4PX(C52) + 8.5% 3PX(C52) + 8.0% 3PX(C48) - 6.1% 4PX(C50) - 5.8% 4PX(C49)
25	+ 13.3% 3PX(C39) + 8.3% 4PX(C39) + 7.8% 3PZ(C39) + 7.0% 2PX(C39) - 5.9% 3PX(O40) + 5.0% 4PZ(C39)
26	+ 6.4% 3PZ(C32) + 4.6% 3PZ(C14) - 4.1% 3PX(C14) + 3.7% 4PX(C36) + 3.5% 3PX(C36) + 3.5% 4PZ(C32)
27	- 11.6% 3PX(C39) - 10.1% 3PZ(C39) - 7.2% 4PX(C39) - 6.4% 4PZ(C39) - 6.1% 2PX(C39) - 5.3% 2PZ(C39)
28	+ 12.9% 4PY(C58) + 12.7% 4PY(C62) + 10.5% 3PY(C62) + 10.3% 3PY(C58) + 5.9% 2PY(C62) + 5.8% 2PY(C58)
29	+ 11.7% 4PY(C64) + 10.2% 3PY(C57) + 9.6% 3PY(C64) + 9.0% 4PY(C57) - 7.6% 4PY(C58) - 6.7% 4PY(C62)
30	+ 11.3% 4PZ(C75) + 10.3% 4PZ(C79) + 8.5% 3PZ(C79) + 8.4% 3PZ(C75) - 5.5% 4PZ(C81) - 5.4% 3PZ(C74)
31	+ 8.7% 4PZ(C74) + 7.9% 4PZ(C78) + 6.5% 3PZ(C78) + 6.3% 3PZ(C74) - 4.0% 3PZ(C73) - 4.0% 4PZ(C80)
32	+ 4.7% 4PZ(C40) + 4.5% 4PZ(C41) + 4.0% 3PZ(C40) + 3.6% 3PZ(C41) + 3.6% 4PX(C40) - 3.6% 4PY(C41)
33	- 14.9% 3PZ(C38) - 9.7% 4PZ(C38) - 7.8% 2PZ(C38) + 7.0% 3PZ(O39) + 4.5% 3S(H30) + 4.3% 2PZ(O39)
34	- 5.7% 4PY(C64) + 5.5% 4PY(C63) + 5.4% 4PY(C67) - 5.2% 4PY(C65) - 4.5% 3PY(C64) + 4.4% 3PY(C67)
35	- 10.9% 3PX(C39) - 6.8% 4PX(C39) - 5.7% 2PX(C39) + 5.0% 3PZ(C39) + 4.9% 3PX(O40) + 3.9% 3S(H31)
36	- 11.7% 3PY(C56) - 7.3% 4PY(C56) - 6.1% 2PY(C56) - 5.8% 3PX(C56) + 5.3% 3PY(O57) - 4.3% 4PX(C56)
37	+ 15.2% 3PX(C28) + 9.8% 4PX(C28) + 7.9% 2PX(C28) + 6.2% 3PZ(C28) - 5.3% 3PX(O29) + 3.4% 2PZ(C28)

Table 6. The results of factor analysis.

Descriptors	E_{HOMO}	E_{LUMO}	ΔE	DM	MV	TNC	η	σ	χ	μ	ω	SEZPE
Factor 1	-.909	.12	.976	-.537	-.859	.93	.971	-.972	.75	-.74	.12	.948
Factor 2	.09	.92	.13	-.357	.10	.09	.20	.13	.659	-.659	.93	0.1

In order to determine which descriptors to be used in the modelling, Genetic Algorithm based fitness function was employed to minimize the squared differences between the observed values and the estimated values of the dependent variable. Hence, four different sets of descriptors are determined. Those sets are denoted in **Table 7**.

Table 7. Four alternative sets of descriptors having minimized function values.

	Sets			
	Set 1	**Set 2**	**Set 3**	**Set 4**
Descriptors	E_{LUMO}	TNC	TNC	TNC
	TNC	DM	μ	ω

Using linear regression model with 20 percent holdout validation, which means that the total data set was randomly split into two non-overlapping sets. While randomly selected 30 molecules, 80 percent of data, was allocated for training set, 7 molecules, 20 percent of data, was used for validation set. The results of the models were summarized in **Table 8**.

According to **Table 8**, model 3 has the highest R^2 and Q^2 scores among others. Hence, the full coefficients of the model are expressed as follows:

$$\log K = 29.540 - 2.172 * TNC + 7.705 * \mu$$

Table 8. Findings related to four alternative models.

	Model			
	1	**2**	**3**	**4**
Descriptors	**TNC and E_{LUMO}**	**TNC and DM**	**TNC and μ**	**TNC and ω**
Coefficients	3.277/-3.085	-3.181/-0.557	-2.172/7.705	-2.781/-5.328
R^2---Q^2 values	0.78---0.80	0.78---0.83	0.81---0.83	0.79---0.81

The factor analysis results for the same molecules whose descriptor values were calculated by B3LYP/6-311++G(2d,2p) method are summarized in **Table 9**.

Table 9. The results of factor analysis.

Descriptors	**E_{HOMO}**	**E_{LUMO}**	**ΔE**	**DM**	**MV**	**TNC**	**η**	**σ**	**χ**	**μ**	**ω**	**SEZPE**
Factor 1	-.931	.046	.966	-.445	-.934	.916	.966	-.965	.830	-.830	.488	.954
Factor 2	.321	.954	-.04	-.454	-.009	-.04	-.04	.04	-.55	.55	-.86	-0.02

While first factor consists of E_{HOMO}, ΔE, MV, TNC, η, σ, χ, μ and SEZPE, the second factor composes of E_{LUMO}, DM and ω. The total variance explained by two factors is 88.37. The data set was split into two non-overlapping sets, which are training set and validation set. While 30 molecules randomly assigned to training set consisting of 80 percent of the data, the rest of the molecules, which is 7, is assigned to validation set accounting for 20 percent of the data set. Genetic Algorithm based minimization function just generates one set of descriptors, which are DM and TNC. Its model is given as follows:

$$\log K = 3.447 - 0.491 * DM - 2.151 * TNC$$

The R^2 and Q^2 values are 0.74 and 0.87, respectively. All calculations were done by SPSS 24.0 and Mat Lab 7.9 software.

4. CONCLUSIONS

A series of 37 polyamino-polycarboxylic ligands for prediction of stability constants of Gd(III) complexes were synthesized and find molecular properties, quantum-chemical calculations by using DFT/B3LYP method with basis sets of the 6-311G(d,p) and 6-311++G(2d,2p). Quantum chemical features such as HOMO, LUMO, HOMO-LUMO energy gap, ionization energy, chemical hardness, chemical softness, electronegativity, chemical potential, dipole moment etc. values for gas phase of neutral molecules were calculated and discussed. According to E_{HOMO} and I results, the electron donating trends for study molecules for gas can be written as for first five molecules: The electron donating trends for study molecules for gas can be written as for first five molecules: 33>30>37>28>31 with B3LYP/6-311G(d,p), and 33>37>28>31>30 with 6-311++G(2d,2p) method. According to energy gap (ΔE), hardness and softness results, the most stable five molecules are found as 1>2>6>20>10 for 6-311G(d,p) and 1>2>6>10>4 for 6-311++G(2d,2p). The most unstable molecules are found as 31, 33 and 37 with 6-311++G(2d,2p) basic set. In general, ΔE values were found with 6-311G(d,p) to be larger than 6-311++G(2d,2p).

4.1. Statistical Conclusion

Two different methods, namely, B3LYP/6-311G(d,p) and B3LYP/6-311++G(2d,2p), are employed to calculate the values of twelve descriptor variables, namely, E_{HOMO}, E_{LUMO}, ΔE, DM, MV, TNC, η, σ, χ, μ, ω and SEZPE. While the first method is used for 37 molecules, the second one is employed for 35 molecules. Those descriptor variables are used to construct models against the values of log K. Before constructing models for each method, those descriptors are factor analysed in order to determine independent set of variables due to existence of co-linearity among them. Then, Genetic Algorithm based minimization function is used in order to determine candidate set of variables in the construction of models. While Genetic Algorithm based minimization, function provides four different sets of variables to choose from since function values are same for the first method, it provides just one set of variables for the second method.

Using those sets of variables generates the better model with the highest R^2 and Q^2 values when compared with others. The linear regression function composes of the descriptors, namely, TNC and μ based on the method called B3LYP/6-311G(d,p). The similar model is constructed based on the method called B3LYP/6-311++G(2d,2p) with descriptors, namely, DM and TNC.

Rererences

[1] De Haenx, C. 2001. Top. Magn. Reson. Imaging, 12, 221-230.
[2] Westbrook, C., Kaut, C. 1998. MRI in Practice, 2th ed, Blackwell Science, 215-218.
[3] Kirchin, M. A., Runge, V. M. 2003. Top. Mag. Res. Ima., 14, 426-435.
[4] Reimer, P., Schneider, G., Schima, W. 2004. Eur. Radiol., 14, 559-578.
[5] Sheppard, D., Allan, L., Martin, P., Mc Leay, T., Milne, W., Houston, J. G. 2004. J. Magn. Reson. Imaging, 20, 256-263.
[6] Frullano, L., Wang, C., Miller, R. H., Wang, Y. 2011. J. Am. Chem. Soc., 133, 1611-1613.
[7] Frullano, L., Zhu, J., Wang, C., Wu, C., Miller, R. H., Wang, Y. 2012. J. Med. Chem., 55, 94-105.
[8] Frullano, L., Zhu, J., Miller, R. H., Wang, Y. 2013. J. Med. Chem., 28, 1629-1640.
[9] Fuchter, M. J., Zhong, C., Zong, H., Hoffman, B. M., Barrett, A. G. M. 2008. Aust. J. Chem., 61, 235-255.
[10] Lee, S., Vesper, B. J., Zong, H., Hammer, N. D., Elseth, K. M., Barrett, A. G. M., Hoffman, B. M., Radosevich, J. A. 2008. Metal-Based Drugs, 30, 3914-3918.
[11] Trivedi, E. R., Vesper, B. J., Weitman, H., Ehrenberg, B., Barrett, A. G. M., Radosevich, J. A., Hoffman, B. M. 2010. Photochem Photobiol, 86, 410-417.
[12] Trivedia, E. R., Ma, Z., Waters, E. A., Macrenaris, K. W., Subramanian, R., Barrettf, A. G. M., Meade, T. J., Hoffman, B. M. 2014. Contrast Media Mol. Imaging, 9, 313-322.
[13] Vlaardingerbroek, M. T., Boer, J. A. 2003. Magnetic Resonance Imaging: Theory and practice; Springer, Verlag: Heidelberg, Germany.
[14] Kiani-Anbouhi, R., Shahabi, S., Ganjali, M. R., Norouzi, P. 2011. Prediction of Gd(III) complexes stability constants for the development of MRI contrast agents, Int. Conf. on Biology, Environment and Chemistry IPCBEE, IACSIT Press, Singapoore, 24, 381-385.
[15] Frisch, M. J.; Trucks, G. W.; Schlegel, H. B.; Scuseria, G. E.; Robb, M. A.; Cheeseman, J. R.; Scalmani, G.; Barone, V.; Mennucci, B.; Petersson, G. A.; Nakatsuji, H.; Caricato, M.; Li, X.; Hratchian, H. P.; Izmaylov, A. F.; Bloino, J.; Zheng, G.; Sonnenberg, J. L.; Hada, M.; Ehara, M.; Toyota, K.; Fukuda, R.; Hasegawa, J.; Ishida, M.; Nakajima, T.; Honda, Y.; Kitao, O.; Nakai, H.; Vreven, T.; Montgomery, J. A., Jr.; Peralta, J. E.; Ogliaro, F.; Bearpark, M.; Heyd, J. J.; Brothers, E.; Kudin, K. N.; Staroverov, V. N.; Kobayashi, R.; Normand, J.; Raghavachari, K.; Rendell, A.; Burant, J. C.; Iyengar, S. S.; Tomasi, J.; Cossi, M.; Rega, N.; Millam, J. M.; Klene, M.; Knox, J. E.; Cross, J. B.; Bakken, V.; Adamo, C.; Jaramillo, J.; Gomperts, R.; Stratmann, R. E.; Yazyev, O.; Austin, A. J.; Cammi, R.; Pomelli, C.; Ochterski, J. W.; Martin, R. L.; Morokuma, K.; Zakrzewski, V. G.; Voth, G. A.; Salvador, P.; Dannenberg, J. J.; Dapprich, S.; Daniels, A. D.; Farkas, Ö.; Foresman, J. B.; Ortiz, J. V.; Cioslowski, J.; Fox, D. J. Gaussian, Inc., Wallingford CT, 2009.
[16] Petersson, G. A., Bennett, A., Tensfeldt, T. G., Al-Laham, M. A., Shirley, W. A., J. Mantzaris, J. 1988. Chem. Phys., 89, 2193-2218.
[17] Becke, A. D. 1993. J. Chem. Phys., 98, 5648-5653.
[18] Costa, J. M., Llush, J. M. 1984. Corros. Sci., 24, 929-933.
[19] Lee, C., Yang, W., Parr, R. G. 1988. Phys. Rev. B, 41, 785-789.
[20] Gorelsky, S. I. 2009. AOMix: Program for molecular orbital analysis, University of Ottawa, Ottawa, Canada, http://www.sg-chem.net.
[21] Gorelsky, S. I., Lever, A. B. P. 201. J. Organomet. Chem., 635, 187-196.
[22] Saracoglu, M., Elusta, M. I. A., Kaya, S., Kaya, C., Kandemirli, F. 2018. Int. J. Electrochem. Sci., 13, 8241-8259.
[23] Kaya, S., Kaya, C., Guo, L., Kandemirli, F., Tüzün, B., Uğurlu, İ., Madkour, L. H., Saracoglu, M. 2016. J. Mol. Liq., 219, 497-504.

[24] Ebenso, E. E., Arslan, T., Kandemirli, F., Love, I., Öğretir, C., Saracoglu, M., Umoren, S. A. 2010. Int. J. Quantum Chem., 110, 2614-2636.
[25] Amin, M. A., Ahmed, M. A., Arida, H. A., Arslan, T., Saracoglu, M., Kandemirli, F. 2011. Corros. Sci., 53, 540-548.
[26] Amin, M. A., Ahmed, M. A., Arida, H. A., Kandemirli, F., Saracoglu, M., Arslan, T., Basaran, M. A. 2011. Corros. Sci., 53, 1895-1909.
[27] Zor, S., Saracoglu, M., Kandemirli, F., Arslan, T. 2011. Corrosion, 67, 125003-1-11.
[28] Kandemirli, F., Saracoglu, M., Bulut, G., Ebenso, E., Arslan, T., Kayan, A. 2012. ITB J. Science (J. Math. and Fund. Sci.), 44A, 35-50.
[29] Amin, M. A., Hazzazi, O. A., Kandemirli, F., Saracoglu, M. 2012. Corrosion, 68, 688-698.
[30] Kandemirli, F., Saracoglu, M., Amin, M. A., Basaran, M. A., Vurdu, C. D., (2014). Int. J. Electrochem. Sci., 9, 3819-3827.
[31] Amin, M. A., El-Bagoury, N., Saracoglu, M., Ramadan, M. 2014. Int. J. Electrochem. Sci., 9, 5352-5374.
[32] Kandemirli, F., Vurdu, C. D., Saracoglu, M., Akkaya, Y., Cavus, M. S. 2015. Int. Res. J. Pure Appl. Chem., 9, 1-16.
[33] El-Bagoury, N., Amin, M. A., Saracoglu, M. 2015. Int. J. Electrochem. Sci., 10, 5291-5308.
[34] İlhan, İ. Ö., Çadır, M., Saracoglu, M., Kandemirli, F., Kökbudak, Z., Akkoç, S. 2015. Chem. Sci. Rev. Lett., 4, 838-850.
[35] Amin, M. A., Fadlallah, S. A., Alosaimi, G. S., Kandemirli, F., Saracoglu, M., Szunerits, S., Boukherroub, R. 2016. Int. J. Hyd. Energy, 41, 6326-6341.
[36] Tazouti, A., Galai, M., Touir, R., Touhami, M. E., Zarrouk, A., Ramli, Y., Saraçoğlu, M., Kaya, S., Kandemirli, F., Kaya, C., 2016. J. Mol. Liquids, 221, 815-832.
[37] Amin, M. A., Saracoglu, M., El-Bagoury, N., Sharshar, T., Ibrahim, M. M., Wysocka, J., Krakowiak, S., Ryl, J. 2016. Int. J. Electrochem. Sci., 11, 10029-10052.
[38] Saracoglu, M., Kandemirli, F., Ozalp, A., Kokbudak, Z. 2017. Chem. Sci. Rev. Lett., 6, 1-11.
[39] Saracoglu, M., Kandemirli, F., Ozalp, A., Kokbudak, Z. 2017. Int. J. Sci. Eng. Inv., 6, 50-57.
[40] Madkour, L. H., Kaya, S., Kaya, C., Guo, L. 2016. J. Taiwan Inst. Chem. Eng., 68, 461-480.
[41] Saracoglu, M., Kandemirli, S. G., Başaran, A., Sayiner, H., Kandemirli, F. 2011. Curr. HIV Res., 9, 300-312.
[42] Saracoglu, M., Kandemirli, F., Amin, M. A., Vurdu, C. D., Cavus, M. S., Sayıner, G. 2015. The Quantum Chemical Calculations of Some Thiazole Derivatives, Proceedings of the 3rd International Conference on Computation for Science and Technology (ICCST-3), Conference Paper, Published by Atlantis Press, 5, 149-154.
[43] Pearson, R. G. 1986. Proc. Natl. Acad. Sci. USA., 83, 8440-8441.
[44] Khaled, K. F. 2010. Electrochim. Acta, 55, 6523-6532.
[45] Pauling, L. 1960. The Nature of the Chemical Bond. Cornell University Press, Ithaca, New York.
[46] Özalp, Z. Kökbudak, M. Saracoglu, F. Kandemirli, İ.Ö. İlhan, C.D. Vurdu, 2015. Chem. Sci. Rev. Lett., 4, 719-728.
[47] Chattaraj, P. K., Sarkar, U., Roy, D. R. 2006. Chem. Rev., 106, 2065-2091.
[48] Ebenso, E. E., Kabanda, M. M., Arslan, T., Saracoglu, M., Kandemirli, F., Murulana, L. C., Singh, A. K., Shukla, S. K., Hammouti, B., Khaled, K. F., Quraishi, M. A., Obot, I. B., Edd, N. O. 2012. Int. J. Electrochem. Sci., 7, 5643-5676.
[49] Musa, A. Y., Kadhum, A. H., Mohamad, A. B., Rohoma, A. B., Mesmari, H. 2010. J. Mol. Struct., 969, 233-237.
[50] Rauk, A. 2001. Orbital interaction theory of organic chemistry. 2rd ed; Wiley Sons, New York, USA.
[51] Obi-Egbedi, N. O., Obot, I. B., El-Khaiary, M. I. 2011. J. Mol. Struct., 1002, 86-96.
[52] Djenane, M., Chafaa, S., Chafai, N., Kerkour, R., Hellal, A. 2019. J. Mol. Struct., 1175, 398-413.
[53] Bhawsar, J., Jain, P., Valladares-Cisneros, M. G., Cuevas-Arteaga, C., Bhawsar, M. R. 2018. Int. J. Electrochem. Sci., 13, 3200-3209.
[54] Obot, I. B., Obi-Egbedi, N. O., Eseola, A. O. 2011. Ind. Eng. Chem. Res., 50, 2098-2110.
[55] Obot, I. B., Obi-Egbedi, N. O., Ebenso, E. E., Afolabi, A. S., Oguzie, E. E. 2013. Res. Chem. Intermed., 39, 1927-1948.
[56] Pearson, R. G. 1963. J. Am. Chem. Soc., 85, 3533-3539.
[57] Bhawsar, J., Jain, P., Valladares-Cisneros, M. G., Cuevas-Arteaga, C., Bhawsar, M. R. 2018. Int. J. Electrochem. Sci., 13, 3200-3209.
[58] Pearson, R. G. 1993. Acc. Chem. Res., 26, 250-255.
[59] Verma, C., Quraishi, M. A., Kluza, K., Makowska-Janusik, M., Olasunkanmi, L. O., Ebenso, E. E. 2017. Sci. Rep., 7, 44432-1-17.
[60] Gece, G. 2008. Corros. Sci., 50, 2981-2992.
[61] Gao, G., Liang, C. 2007. Electrochim. Acta, 52, 4554-4559.
[62] Sahin, M., Gece, G., Karci, F., Bilgic, S. 2008. J. Appl. Electrochem., 38, 809-815.
[63] Quraishi, M. A., Sardar, R. 2003. J. Appl. Electrochem., 33, 1163-1168.
[64] Kaya, S., Banerjee, P., Saha, S. K., Tüzün, B., Kaya, C. 2016. RSC Adv., 6, 74550-74559.
[65] Khaleda, K. F., Al-Qahtani, M. M. 2009. Mater. Chem. Phys., 113, 150-158.
[66] Guan Luo, Y. C., Han, K. N. 1998. Corrosion, 54, 721-731.

[67] Martinez, S., Štagljar, I. 2003. J. Mol. Struct. (THEOCHEM), 640, 167-174.
[68] Gece, G., Bilgiç, S. 2009. Corros. Sci., 51, 1876-1878.